10 The Berezinskii-Kosterlitz-Thouless Transition and its Application to Superconducting Systems

Lara Benfatto
Sapienza University of Rome
P.le A. Moro 5, 00185 Rome, Italy

Contents

E. Pavarini and E. Koch (eds.)
Correlations and Phase Transitions
Modeling and Simulation Vol. 14
Forschungszentrum Jülich, 2024, ISBN 978-3-95806-751-6
http://www.cond-mat.de/events/correl24

1 Introduction

Almost 50 years after the seminal work by Berezinskii [1] and Kosterlitz and Thouless [2] the Berezinskii-Kosterlitz-Thouless (BKT) transition remains one of the most fascinating examples of topological phase transitions in condensed-matter system, and as such it has been acknowledged by the 2016 Nobel Prize in Physics. Its universality class describes several phenomena ranging from the quantum metal-insulator transition in one dimension to the Coulomb-gas screening transition in 2D, and of course the metal-to-superfluid transition in 2D [3]. As such it has been investigated in neutral superfluids, as, e.g., thin He films [4,5] and cold-atoms systems made of bosons [6] or neutral fermions [7]. Nonetheless, despite the fact that in the original paper by Kosterlitz and Thouless [2] the authors argued that the BKT transition should not be observed in (quasi) two-dimensional (2D) superconductors, this is certainly the field where it has been most widely discussed. As we will see in this Chapter, the conditions under which BKT physics can be seen in quasi-2D superconductors are not always met. Nonetheless, in the past and recent literature the BKT physics has been invoked to explain observations in a wide class of systems: thin films of conventional [8–10] and unconventional [11–13] superconductors, but also to the 2D electron gas confined at the interface between two insulators in artificial heterostructures [14–16], or in the top-most layer of ion-gated superconducting (SC) systems [17]. Due to the breadth of literature on the subject, the references provided in the present lecture cannot be at any extent exhaustive: the reader must be conscious that they just reflect the personal choice of the author in providing few (over many) examples for each category of problems that will be discussed.

The aim of this lecture is twofold. From one side, I will provide a general introduction to the basic theoretical concepts behind the understanding of the BKT transition, and from the other side I will summarize the efforts done over the years to understand how one can measure and interpret experimental signatures of BKT physics in real materials, especially superconductors.

For the first part, I will start from the description of the BKT transition within the classical XY-model, which describes Heisenberg interactions between two-component classical spins in a 2D lattice. The physical transition behind this model is then the paramagnetic-ferromagnetic transition in 2D, and it allows one to understand easily the basic difference between "order" and "spin rigidity" that is at the heart of the BKT physics. In addition, it allows one to easily visualize the topological excitations as spin vortices that appear in 2D in addition to the more conventional spin waves. As a second step, I will show the formal mapping between this problem and the screening transition for the Coulomb gas, always in 2D. This analogy allows one to grasp an intuition on the role of vortices to break the "quasi-long-range" order of the low-temperature phase as an effect analogous to the screening of Coulomb interaction by charges that are free to move. Finally, I will also mention the mapping into the sine-Gordon model, that describes again a completely different physical problem, i.e., a quantum field in one dimension. Such a mapping turns out to provide an alternative, elegant way to derive the renormalization-group equations of the BKT transition via quantum-field theory techniques, as beautifully described in the book by T. Giamarchi [18], that is also rather powerful to describe the role played by

screening currents in a charged superfluid [19, 20].
For the second part, I will discuss to what extent the BKT transition can be observed in superconductors, and what we can define as "2D superconductors" within the context of BKT physics. I will then discuss in detail the benchmark experimental determination of the BKT transition, i.e., the well-known BKT universal jump of the superfluid density [21], that has been beautifully confirmed few years after the theoretical prediction by Nelson and Kosterlitz by experiments in He films [5]. After a critical discussion of *what* exactly "universal jump" means within the context of experiments in superconductors, as compared to the case of neutral superfluids, I will review the results of the last ten years or so to identify this signature in real systems. As we shall see, in most of the hypothetical quasi-2D superconductors where a BKT jump could be expected it appears somehow hidden by *inhomogeneity* effects, that systematically smear it out, hindering its observation. Nonetheless, I will present few paradigmatic cases where BKT physics seems to be supported by the experiments, once the "textbook" results are properly analyzed by taking into account the role of inhomogeneity. In the last Section I will also discuss two other celebrated examples of experimental observations of BKT physics connected to vortex transport, i.e., the non-linear I-V characteristics below T_{BKT} and the exponential temperature dependence of the paraconductivity above T_{BKT} [22]. Also in these cases I will point out physical effects present in real materials that can overscreen a pure BKT phenomenon, requiring a careful analysis of the experimental conditions under which BKT physics can be disentangled from other phenomena.

2 The XY-model

The pioneering works of Berezinkii [1] and Kosterlitz and Thouless [2] in the late 70's were originally motivated by the ongoing discussion at the time on the possibility to observe some sort of transition in 2D, that could be still consistent with the expectation of the Mermin-Wagner theorem [23]. The Mermin-Wagner theorem states that a 2D system cannot break spontaneously a continuous symmetry at finite temperature. The reason, as we shall see below via an explicit computation, is that the thermal fluctuations of the Goldstone (massless) mode which emerges when a continuous symmetry is broken completely spoil the order parameter of the transition itself. At that time, the contribution of Berezinkii from one side, and Kosterlitz and Thouless from the other, was to shown that a phase transition can still take place, but it must be identified by starting from a more general definition of "quasi-ordered" state, that is no more characterized by a finite order parameter, but rather by a finite "rigidity" of the state itself. Once established that a phase transition can be identified on the basis of the presence (below T_{BKT}) or the absence (above T_{BKT}) of rigidity, they showed that topological vortex-like excitations play a central role in driving the transition. It must be noted that the concept of rigidity as manifestation of a phase transition is not limited to the BKT case. Just to mention the most intuitive case, when translational symmetry is broken to form a solid the system becomes indeed "rigid" (we can walk on it!). The Goldstone modes of the transition in this case are the acoustic phonons, whose energy scales with the gradient of the lattice deformation. As such, as the wavelength of the deformation goes to infinity, i.e., the momentum goes to zero, it cost nothing to create the phononic distortion, i.e., the mode appears "massless". This analogy will be useful to understand the results we will derive in this Section.

To start the discussion on the basic concepts behind the BKT transition let us introduce the XY-model, where these effects were originally discussed. The model describes the ferromagnetic interactions between planar spins with fixed modulus ($|\mathbf{S}_i| = 1$), placed on a square lattice. Its Hamiltonian reads

$$H_{XY} = -J\sum_{\langle i,j\rangle} \mathbf{S}_i \cdot \mathbf{S}_j = -J\sum_{\langle ij\rangle} \cos\big(\theta_i - \theta_j\big), \tag{1}$$

where the sum $\sum_{\langle i,j\rangle}$ is restricted to nearest neighbors spins, J is a positive coupling constant and θ represents the angle that each spin form with the x direction. For convenience of language, and for the sake of the analogy with the role played by θ within the context of the superfluid transition, we will refer to it as to a "phase" variable. From (1), it is straightforward to recognize that the system shows two different symmetries

- q continuous and global symmetry $U(1)$: $\quad \forall i : \theta_i \to \theta_i + c$
- q discrete and local symmetry $\mathbb{Z}^m$: $\quad \theta_i \to \theta_i + 2\pi m$

In the following, we will see that these two symmetries are connected to two different phase excitations below T_{BKT}. Let us start to analyze the Hamiltonian (1) trying to guess the low-temperature ground state. It can be easily understood that the minimum value of the energy corresponds to a situation in which all the spins are aligned in one particular direction, say θ_i=0 for all spins, breaking in this way the $U(1)$ symmetry of the Hamiltonian itself. Whenever this happens, the system has a finite macroscopic magnetization in the x direction, i.e. $\langle \mathbf{S}\rangle = \hat{x}$. Let us see why this is not possible, as expected on the basis of the Mermin-Wagner theorem.

At finite temperature, the phase θ_i of each site can fluctuate with respect to the ground-state value. We are interested in computing the contribution of such phase fluctuations to $\langle \mathbf{S}\rangle$ in a low-temperature phase, where the difference in phase between neighboring spins is very small, so that we can rewrite the Hamiltonian (1) by expanding the cosine up to the second order in its argument. Furthermore, by taking the continuum limit on the lattice we can approximate $\theta_i - \theta_{i+\hat{\delta}} \approx a\,\partial\theta(\mathbf{r})/\partial\hat{\delta}$, where $\theta(\mathbf{r})$ is a smooth function and $\hat{\delta} = x, y$. Finally, we get

$$H_{XY} \simeq \frac{J}{2}\int d\mathbf{r}\,\big(\nabla\theta(\mathbf{r})\big)^2 = \frac{J}{2}\int \frac{d\mathbf{q}}{(2\pi)^2}\,\mathbf{q}^2\,|\theta_{\mathbf{q}}|^2. \tag{2}$$

Thanks to the Gaussian approximation (2) to the XY-Hamiltonian we can easily compute the effect of phase fluctuations as

$$\langle \mathbf{S}_i\rangle = \big\langle e^{i\theta_i}\big\rangle = e^{-\langle\theta_i^2\rangle/2}\,, \tag{3}$$

where in the last passage we have used a well known property of the average over a Gaussian distribution (see Appendix A), while the average $\langle\cdots\rangle$ is defined as the average over the canonical ensemble of the system

$$\langle A\rangle = \frac{1}{Z}\int_0^{2\pi} d\theta_1 \cdots \int_0^{2\pi} d\theta_N\, A e^{-\beta H_{XY}}, \tag{4}$$

where as usual $\beta = 1/T$. By using the approximation (2) the calculation (3) is straightforward

$$\langle \theta_i^2 \rangle = \int \frac{d\mathbf{q}}{(2\pi)^2} \langle |\theta_{\mathbf{q}}|^2 \rangle = \int_{1/L}^{1/a} \frac{d\mathbf{q}}{(2\pi)^2} \frac{T}{J\mathbf{q}^2} = \frac{T}{2\pi J} \ln \frac{L}{a}\,, \tag{5}$$

where we used the fact that from Hamiltonian (2)

$$\big\langle \theta_{\mathbf{q}_1} \theta_{\mathbf{q}_2} \big\rangle = \frac{T}{J\mathbf{q}_1^2}\, \delta_{\mathbf{q}_1,-\mathbf{q}_2}, \tag{6}$$

and we denoted with L the linear size of the system and with a the lattice spacing between two neighboring spins. Substituting the result (5) into Eq. (3) we get

$$\langle \mathbf{S}_i \rangle = e^{-\frac{T}{4\pi J}\ln(L/a)} = \Big(\frac{a}{L}\Big)^{\frac{T}{4\pi J}} \xrightarrow[L\to\infty]{} 0\,. \tag{7}$$

Hence, at any nonzero temperature the system cannot sustain a spontaneous magnetization in the thermodynamic limit, since the spin wave excitations suppress the long-range order. As one can immediately see from Eq. (2), spin waves appear as smooth variations of the phase, that cost no energy in the long-wavelength ($\mathbf{q} \to 0$) limit. Thus, in the 2D XY-model they are indeed "massless" at long-wavelength, and as such they can be recognized as the Goldstone modes of the system. We then proved explicitly the Mermin-Wagner theorem.
However, it is worth to mention that very often real systems are quite far from the thermodynamic limit so that they could exhibit a finite magnetization in the low-temperature regime. Indeed, if we estimate the exponent of (7), using the universal relation between the renormalized stiffness J and the temperature at the critical point (we will come back on this point in the next pages), we obtain that it is $\leq 1/8$. It means that for a microscopic scale $a \sim 10$ nm one would need a system with a linear size $L \sim 100000$ km to have $\langle \mathbf{S}_i \rangle = 0.01$. In short, if a real finite system exhibits a spontaneous symmetry breaking, it does not mean that the Mermin Wagner theorem is violated, but that the system studied is far away from its thermodynamic limit.
Anyway, at the time of its formulation, the generally accepted conclusion was that in the XY-model[1] there is no transition to an ordered state at any nonzero temperature. The merit of Berezinskii, Kosterlitz and Thouless was first of all to overcome this idea, by realizing that a different kind of transition was possible.

2.1 Correlation functions and rigidity

Even though we have explicitly seen that a conventional order-parameter description of the phase transition is not possible, since $\langle \mathbf{S}_i \rangle = 0$ at any temperature, the close investigation of the behavior of the spin correlation functions suggests that a change of behavior should still happen between the low and high-temperature phase. The correlation function between two sites i and j is defined as

$$C(\mathbf{r}_i - \mathbf{r}_j) = \big\langle \mathbf{S}_i \cdot \mathbf{S}_j \big\rangle = \big\langle \cos(\theta_i - \theta_j) \big\rangle. \tag{8}$$

[1]More generally in a two-dimensional system with a continuous symmetry and short-range interactions.

Let us try to estimate its behavior in the low-temperature $\beta J \ll 1$ and high temperature limit $\beta J \ll 1$, respectively. At low temperature we can rely on the same approximated Gaussian Hamiltonian (2) used above for the calculation of the average order parameter. Using again the properties of Gaussian averages we get

$$C(\mathbf{r}) = \left\langle e^{i(\theta(\mathbf{r})-\theta(0))} \right\rangle = e^{-\frac{1}{2}\left\langle \theta(\mathbf{r})-\theta(0)^2 \right\rangle}, \tag{9}$$

where the quantity in the exponent is computed in Fourier space as

$$\begin{aligned} \left\langle(\theta(\mathbf{r})-\theta(0))^2\right\rangle &= \left\langle \int \frac{d\mathbf{q}_1}{2\pi}\,\theta_{\mathbf{q}_1}\left(e^{i\mathbf{q}_1\mathbf{r}}-1\right)\int \frac{d\mathbf{q}_2}{2\pi}\,\theta_{\mathbf{q}_2}\left(e^{i\mathbf{q}_2\mathbf{r}}-1\right)\right\rangle = \int \frac{d\mathbf{q}}{(2\pi)^2}\left(2-2\cos(\mathbf{q}\cdot\mathbf{r})\right)\left\langle|\theta(\mathbf{q})|^2\right\rangle \\ &= \frac{T}{\pi J}\left(\int_{1/L}^{1/a}\frac{dq}{q}\left(1-\cos(\mathbf{q}\cdot\mathbf{r})\right)\right) \sim \frac{T}{\pi J}\int_{1/r}^{1/a} dq\,\frac{1}{q} = \frac{T}{\pi J}\ln\frac{r}{a}, \end{aligned} \tag{10}$$

where the result (6) for the phase correlation function of the Gaussian model has been used. Finally, by substituting this result in Eq. (9) we obtain

$$C(\mathbf{r}) = e^{-\frac{T}{2\pi J}\ln(r/a)} = \left(\frac{a}{r}\right)^{\frac{T}{2\pi J}}. \tag{11}$$

In the high-temperature regime one can attempt an estimate of the correlation function in power law of the small parameter $\beta J \ll 1$. In this regime one is not authorized to assume small fluctuations of $\theta_i - \theta_j$, and in general the full cosine structure of Eq. (1) should be retained, along with its periodicity modulo 2π. The details of this calculation can be found in Ref. [24]. The final result is that the correlation function decays in this regime exponentially, with a correlation length ξ depending on the temperature

$$C(\mathbf{r}_i - \mathbf{r}_j) \simeq e^{-|\mathbf{r}_1-\mathbf{r}_2|/\xi}, \quad \xi = \ln\frac{2T}{J}. \tag{12}$$

Let us compare the results (11) and (12) with the standard expectations for a second-order phase transition according to Landau theory. Denoting with $m = \langle \mathbf{S} \rangle$ the average order parameter below T_c, one usually finds

$$C(\mathbf{r}) \simeq \quad A e^{-\mathbf{r}\xi_+}, \quad T > T_c \tag{13}$$

$$C(\mathbf{r}) \simeq \quad m^2 + B e^{-\mathbf{r}\xi_-}, \quad T < Tc \tag{14}$$

where A, A' are constants, and the correlation length above ξ_+ and below ξ_- both diverge as T_c is approached as

$$\xi_\pm(T) \sim \frac{1}{|T-T_c|^\nu}, \quad T \to T_c, \tag{15}$$

with $\nu = 1/2$ in the mean-field case. In other words, the correlation function for the observable that represents the order parameter decays exponentially to zero in the disordered state, while it tends exponentially to the square of the order parameter in the ordered state. The results found above for the XY-model are radically different: at high temperature we recover indeed an exponential decay to zero, Eq. (12), but the correlation length does not diverge at any finite temperature. On the other hand, in the low-temperature expansion (11) the correlation length tends to zero with a power-law instead of an exponential behavior. Strictly speaking, such a scaling implies that $\xi \to \infty$ in the ordered state. Observe also that both results are consistent with the Mermin-Wagner theorem: the system does not display a non-zero order parameter at any finite temperature. On the other hand, such a drastic change of behavior of the correlation functions cannot occur without the emergence of a phase transition in between: the transition in this case cannot be characterized by a vanishing of the order parameter (that is always zero at finite temperature in the thermodynamic limit), but by the change of scaling of the system correlation functions. At low temperature, the long-wavelength spin fluctuations, or spin waves, have a finite spin (or phase) stiffness, encoded in the finite coefficient of the $(\nabla\theta)^2$ term of Eq. (2). The direct consequence of this rigidity against phase fluctuations is the (weak) power-law decay of correlation functions at large distances, encoded into Eq. (11). On the other hand, at high temperature, a full cosine-like interaction term should be considered in the Hamiltonian, and the system recovers a standard exponential decay (12) of the correlation function, and the phase rigidity, that controls the power-law decay of the low-temperature expansion (11), is lost. To understand how this transition occurs, we must take into account vortices, not considered so far.

2.2 The role of vortices

Let us tackle the problem starting from the low-temperature expansion (2). It is clear that this approximation cannot be the end of the story: the model (2) is purely Gaussian, and as such it cannot induce any transition. On the other hand, as emphasized above, the pure exponential decay (12) of the correlation functions can only be recovered by retaining the full cosine structure of the Hamiltonian. As a consequence, one recognizes that while going from the original model (1) to the approximated one (2) we have lost one important *discrete* symmetry of the original XY-model, mentioned at the beginning: the invariance under a *local* transformation

$$\theta_i \to \theta_i \pm 2\pi m\,, \tag{16}$$

with $m \in \mathbb{Z}$, for each site i of the lattice. The presence of this discrete symmetry leads to the existence of a new kind of phase excitations that are topological in character and cannot be smoothly connected to the unperturbed ground state. These are vortices, characterized by a winding of the phase by $\pm 2\pi$ by going around their center

$$\oint \nabla\theta \cdot d\vec{\ell} = 2\pi n\,. \tag{17}$$

It is clear that if a vortex excitation is present in the system, one cannot make the assumption of smoothness of the phase variations in neighboring sites, that led us to the approximate form (2). Thus, vortices are good candidates to be responsible for the phase transition we are looking for. The question to be answered is then: how much energy does it cost to introduce a vortex in the system? Indeed, the answer to this question can also help us understanding what is the temperature scale where the vortex proliferation occurs.

To make this estimate we would like to keep the continuum notation for $\theta(\mathbf{r})$ but allowing also for configurations that are singular in a position $\mathbf{r}_0$. The easiest way to introduce vortices into the low-temperature model (2) is to assume that the Gaussian Hamiltonian admits both *smooth* solutions θ_{SW}, that represent the longitudinal spin waves, and *singular* solutions θ_V, which represent vortices. These two solutions are obtained by a variational principle applied to the Hamiltonian (2): the variational equation $\delta H = 0$ reads in general

$$\nabla^2\theta(\mathbf{r}) = 0. \tag{18}$$

We will then describe spin-waves as solutions of Eq. (18) in all space, and vortices as solutions that satisfy Eq. (18) everywhere except than in isolated points, that represent the vortex center

$$\begin{aligned} \nabla^2\theta_{SW}(\mathbf{r}) &= 0\,, \qquad (19)\\ \nabla^2\,\theta_V(\mathbf{r}) &= 2\pi q\,\delta(\mathbf{r}-\mathbf{r}_0), \qquad (20)\end{aligned}$$

where q is an integer (positive or negative) number representing the vorticity of the topological excitation at $\mathbf{r}_0$. The solution of Eq. (20) for $q = 1$ in 2D is exactly

$$\theta_V = \arctan\frac{y-y_0}{x-x_0}\,, \tag{21}$$

that is the configuration of a vortex. Indeed, since $\nabla\theta_V = \big(-(y-y_0),\, x-x_0\big)/R^2$, with $R=|\mathbf{r}-\mathbf{r}_0|$, one immediately sees that by computing, e.g., Eq. (17) along a circle of radius R around $\mathbf{r}_0$ that $\nabla\theta_V \parallel \vec{d\ell}$, so that from Eq. (17) we get

$$\oint \nabla\theta_V\cdot\vec{d\ell} = \frac{1}{R}\oint d\ell = \frac{1}{R}\,2\pi R = 2\pi\,. \tag{22}$$

By inserting the solution (21) into the Hamiltonian (2) we can then calculate the energy of the vortex configuration as

$$E = \frac{J}{2}\int d\mathbf{r}\big(\nabla\theta_V(\mathbf{r})\big)^2 = \frac{J}{2}\int_a^L dr\,2\pi r\frac{1}{r^2} = \pi J\ln\frac{L}{a}\,, \tag{23}$$

where we used the fact that the distance R from the vortex center is limited below by the lattice spacing and above by the system size L. This energy is diverging logarithmically with the system size L, disfavoring the generation of vortices in the thermodynamic limit. However, at finite temperature we must consider also the gain in entropy in forming the vortex configuration. Since the number of independent places where a vortex can be located is $\sim L^2/a^2$, we obtain that also the entropy has a logarithmic dependence on the system size

$$S = \ln\frac{L^2}{a^2} = 2\ln\frac{L}{a}\,. \tag{24}$$

In conclusion we have that the free energy of a vortex configuration is

$$F = E - TS = \big(\pi J - 2T\big)\ln\frac{L}{a}\,, \tag{25}$$

so that as soon as

$$T > T_{BKT} = \frac{\pi J}{2}\,, \tag{26}$$

the emergence of an isolated vortex is entropically convenient. Even though we did not prove it yet, it is physically plausible that when vortices proliferate they destroy the quasi-long-range order encoded in the power-law correlation functions (11). More precisely, we will demonstrate, by means of the renormalization-group equations, that the phase rigidity goes to zero. It is worth stressing where the dimensionality entered crucially in the above argument. The entropic cost to obtain a vortex is always logarithmically increasing with the system size, as in Eq. (24) above. However, in dimensions larger than two the energetic cost of vortex configuration would scale faster than $\log(L)$, making the energy term always predominant over the entropic one. Thus, unless additional effects enter to cut-off at large distance the energetic cost of a vortex (as it happens, e.g., in charged superconductors [25]) the free energy of a vortex configuration cannot spontaneously change sign as temperature increase.

The above argument is the one provided in the original paper by Kosterlitz and Thouless [2]. Even though it is qualitatively correct, it neglects two effects. (i) While going from the lattice to the continuum model one misses the energetic costs to form the vortex at the length-scale of the lattice spacing. This energy, that is usually referred as vortex-core energy μ, is a constant that must be added in Eq. (23). Even though it does not change considerably the estimate (26), where only the terms growing with the system size are relevant, it can be nonetheless relevant if one wants to make a direct comparison with experimental data in real superconducting systems, as we will discuss extensively below. (ii) We estimated the transition temperature by considering a single vortex with infinite size, while the reality could be more complicated, with several vortex excitations occurring on shorter scales. For example, if one puts a vortex at $\mathbf{r}_+$ and an antivortex (with same vorticity) at $\mathbf{r}_-$, at scales larger than $\sim |\mathbf{r}_+ - \mathbf{r}_-|$ the phase configuration remains unperturbed. In the spirit of Eq. (23), the log divergence of the integral is cut-off at a scale or order $|\mathbf{r}_+ - \mathbf{r}_-|$. This implies that such vortex "pairs" are energetically possible also below T_c, and can change the "effective" large-distance J that enters Eq. (26). These additional effects are beautifully explained, as we shall see in the next sections, by the renormalization group (RG) analysis of the BKT transition, that was developed by Kosterlitz [26] right after the publication of the original paper with Thouless. The starting point to carry on this analysis was the explicit construction of the mapping into the Coulomb-gas problem, that we will discuss in the next section.

3 Mapping to the Coulomb-gas and sine-Gordon model

As we discussed in the previous Section, vortex-like fluctuations can be introduced into the Gaussian model (2) by allowing for singular solutions (20) of the $\delta H = 0$ variational equation. We can try to pursue this analogy further by writing down a model that also includes interactions between vortices, mediated by spin-wave excitations. This is the idea that was followed by Kosterlitz [26] to write down a partition function for multiple vortices, to be further studied by means of the RG approach. It turns out that the Hamiltonian describing interactions between vortices is formally equivalent to the Hamiltonian of the Coulomb gas in two dimensions. I will review here in detail the derivation of the mapping, as it is discussed in [24], since it allows one to grasp several aspects of the vortex physics, besides providing an additional example of a completely different problem (the screening transition for the 2D Coulomb gas) that still belongs to the BKT universality class.

Let us start again from the low-temperature model (2) and let us promote the phase gradient to a generic current density $\mathbf{j}$

$$\nabla\theta \;\Rightarrow\; \mathbf{j}\,, \tag{27}$$

so that the Hamiltonian (2) becomes more generally

$$H = \frac{J}{2}\int d\mathbf{r}\,\mathbf{j}^2(\mathbf{r}). \tag{28}$$

Such a terminology is further motivated by the application to the case of superconductors, where $\nabla\theta$ is directly connected to the physical electronic current density in the SC state (see Eq. (64) below). In full generality, we can always decompose $\mathbf{j}$ in its longitudinal $\mathbf{j}_{\parallel}$ and transverse $\mathbf{j}_{\perp}$ components, defined as usual as

$$\mathbf{j} = \mathbf{j}_{\parallel} + \mathbf{j}_{\perp} \quad \text{with} \quad \nabla\times\mathbf{j}_{\parallel} = 0 \quad \text{and} \quad \nabla\cdot\mathbf{j}_{\perp} = 0\,. \tag{29}$$

By close inspection of the spin-wave (19) and vortex-like (20) phase excitations we also realize that the former are connected to the longitudinal component, while the latter represent the transverse components. Indeed we see that only $\mathbf{j}_{\perp}$ contributes to vortices, since

$$\oint \mathbf{j}\cdot d\vec{\ell} = \int_S (\nabla\times\mathbf{j})\cdot d\mathbf{s} = \int_S (\nabla\times\mathbf{j}_{\perp})\cdot d\mathbf{s} = 2\pi\sum_i q_i\,, \tag{30}$$

where q_i is an integer (positive or negative number) defining the vorticity of the i-th vortex. Eq. (30) is a generalization of Eq. (22) in the case where several vortices with different vorticity are present. The longitudinal and transverse components can be defined in terms of scalar functions as

$$\mathbf{j}_{\parallel} = \nabla\theta_{SW} \quad \text{and}\; \mathbf{j}_{\perp} = \nabla\times(\hat{z}W) = \big(\partial_y W,\, -\partial_x W,\, 0\big). \tag{31}$$

In this way we also have that $\nabla\times\mathbf{j}_{\perp} = \big(0,\,0,\,-\nabla^2 W\big)$. Inserting this relation into Eq. (30) we then conclude that W must satisfy the equation

$$\nabla^2 W(\mathbf{r}) = -2\pi\rho(\mathbf{r}), \tag{32}$$

$$\rho(\mathbf{r}) = \sum_i q_i\,\delta(\mathbf{r}-\mathbf{r}_i). \tag{33}$$

Eq. (32) is exactly the Poisson equation in 2D for the potential W generated by a distribution of point-like charges q_i at the positions $\mathbf{r}_i$. Its solution is in general

$$W(\mathbf{r}) = 2\pi\int d\mathbf{r}'\,V(\mathbf{r}-\mathbf{r}')\rho(\mathbf{r}'), \tag{34}$$

where $V(\mathbf{r})$ is the Green's function of the Poisson equation, i.e., the solution of the homogeneous equation (corresponding to the Coulomb potential in 2D) that reads

$$\nabla^2 V(\mathbf{r}) = -\delta(\mathbf{r}) \quad \Rightarrow V(\mathbf{r}) = \int \frac{d\mathbf{k}}{(2\pi)^2} \cdot \frac{e^{i\mathbf{k}\cdot\mathbf{r}}}{\mathbf{k}^2}. \tag{35}$$

Notice that here we denote as Coulomb potential in 2D the Fourier transform of $1/\mathbf{k}^2$ in two spatial dimensions, so that we obtain $V(r) \simeq -\ln r$ at large distances, instead of the usual $1/r$ of the 3D case. If we use the decomposition (29) in Eq. (28) we immediately see that the mixed terms vanishes since $\int d\mathbf{r}\, \mathbf{j}_\parallel \cdot \mathbf{j}_\perp = \int d\mathbf{r}\, \nabla\theta_L \cdot \big(\nabla\times(\hat{z}W)\big) = \theta_L\big(\nabla\times(\hat{z}W)\big)\cdot \hat{n}_S\big|_{\partial S} = 0$, since the integration surface S can be taken larger than the sample area, leading to a vanishing current at the border ∂S. As a consequence, we obtain that longitudinal and transverse degrees of freedom decouple $H = H_\parallel + H_\perp$, and we can focus on the term $H_\perp = (J/2)\int d\mathbf{r}\, \mathbf{j}_\perp^2$ that describes the interaction between vortices. Thanks to the result (34) it can be written as

$$\begin{aligned} H_\perp &= \frac{J}{2}\int d\mathbf{r}\, \mathbf{j}_\perp^2 = \frac{J}{2}\int d\mathbf{r}\big(\nabla\times(\hat{z}W)\big)^2 = \frac{J}{2}\int d\mathbf{r}\big(\nabla W\big)^2 = -\frac{J}{2}\int d\mathbf{r}\, W\nabla^2 W \\ &= \pi J\int d\mathbf{r}\, W(\mathbf{r})\rho(\mathbf{r}) = 2\pi^2 J\int d\mathbf{r} d\mathbf{r}'\rho(\mathbf{r})V(\mathbf{r}-\mathbf{r}')\rho(\mathbf{r}') = 2\pi^2 J\sum_{ij} q_i q_j V(\mathbf{r}_i-\mathbf{r}_j). \end{aligned} \tag{36}$$

Eq. (36) expresses the interaction energy between vortices in the same form of the electrostatic energy of point-like charges q_i, leading to a global charge density $\rho(\mathbf{r})$, interacting via a 2D Coulomb potential $V(\mathbf{r})$. An interesting outcome of the derivation (36) is that, due to the divergence of the potential $V(\mathbf{r})$ as $r \to 0$, only neutral configurations contribute to the partition function. If we compute $V(\mathbf{r})$ from Eq. (35) we see that at the shortest scale of the system, i.e., when we put two vortices on the same site, it has a contribution diverging with the system size

$$V(r{=}0) = \int_{1/L}^{1/a} dk\, \frac{1}{2\pi k} = \frac{1}{2\pi}\ln\frac{L}{a} \to \infty \quad \text{for } L \to \infty. \tag{37}$$

It we separate this divergent term by defining

$$V(\mathbf{r}) = V(0) + G(\mathbf{r}), \tag{38}$$

where now $G(\mathbf{r}{=}0) = 0$, in Eq. (36) we obtain

$$2\pi^2 J\sum_{ij} q_i q_j\big(V(0)+G(\mathbf{r}_i-\mathbf{r}_j)\big) = 2\pi^2 J V(0)\Big(\sum_i q_i\Big)^2 + 2\pi^2 J\sum_{ij} q_i q_j G(\mathbf{r}_i-\mathbf{r}_j). \tag{39}$$

Since the Boltzmann weight of each configuration is $e^{-\beta H_\perp}$ the divergence of $V(0)$ in the thermodynamic limit leads to a vanishing contribution to the partition function, unless

$$\sum_i q_i = 0. \tag{40}$$

Using the neutrality condition (40) and the fact that $G(0) = 0$, the last term of Eq. (39) can be written as

$$2\pi^2 J\sum_{ij} q_i q_j G(\mathbf{r}_i-\mathbf{r}_j) = 2\pi^2 J\sum_i q_i^2 G(r{=}0) + 2\pi^2 J\sum_{i\neq j} q_i q_j G(\mathbf{r}_i-\mathbf{r}_j) = 2\pi^2 J\sum_{i\neq j} q_i q_j G(\mathbf{r}_i-\mathbf{r}_j), \tag{41}$$

such that $\mathbf{r}_i - \mathbf{r}_j$ in the last term is at least of order of the lattice spacing. The precise form of the function $G(\mathbf{r})$ follows from the evaluation of the integral (35) on the lattice, that allows one to define the energetic cost to create the vortex on the shortest scale $r = a$. More specifically, one can promote the continuum gradient into a discrete one, and define the Fourier transform of the potential as $V(\mathbf{k}) = a^2/\big(4-2\cos k_x a - 2\cos k_y a\big)$, that reduces to $V(\mathbf{k}) \sim 1/\mathbf{k}^2$ as $ka \ll 1$. From such a discretization the $G(|\mathbf{r}|{=}a)$ potential reads

$$\begin{aligned} G(\mathbf{r}{=}a\hat{x}) = V(\mathbf{r}{=}a\hat{x}) - V(0) &= \int \frac{d^2\mathbf{k}}{(2\pi)^2}\big(e^{i\mathbf{k}\cdot\mathbf{r}}-1\big)V(\mathbf{k}) = \int \frac{d^2\mathbf{k}}{(2\pi)^2}\,\frac{a^2\big(\cos k_x a - 1\big)}{4-2\cos k_x a - 2\cos k_y a} \\ &= \frac{1}{2}\int \frac{d^2\mathbf{k}}{(2\pi)^2}\,\frac{a^2\big(\cos k_x a + \cos k_y a - 2\big)}{4-2\cos k_x a - 2\cos k_y a} = -\frac{1}{4}\,. \end{aligned} \tag{42}$$

This result allows us to rewrite the $G(\mathbf{r})$ potential at the scale relevant for Eq. (41) as

$$G\big(r \gtrsim a\big) \simeq -\frac{1}{4} - \frac{1}{2\pi}\ln\Big(\frac{r}{a}\Big), \tag{43}$$

so that Eq. (36) can be written as

$$\begin{aligned} H_\perp &= 2\pi^2 J \sum_{i\neq j} q_i q_j G(\mathbf{r}_i - \mathbf{r}_j) = -2\pi^2 J \sum_{i\neq j}\left(\frac{1}{4} + \frac{1}{2\pi}\ln\frac{r_{ij}}{a}\right) q_i q_j \\ &= -\frac{\pi^2 J}{2}\sum_{i\neq j} q_i q_j - \pi J \sum_{i\neq j} q_i q_j \ln\frac{r_{ij}}{a} = \mu \sum_i q_i^2 - \pi J \sum_{i\neq j} q_i q_j \ln\frac{r_{ij}}{a}\,, \end{aligned} \tag{44}$$

where we used $\sum_{i\neq j} q_i q_j {=} -\sum_i q_i^2$ from Eq. (40) and identified the vortex-core energy μ with

$$\mu \equiv \mu_{XY} = \frac{\pi^2 J}{2}\,. \tag{45}$$

Finally, we can use the neutrality condition (40) by imposing that vortices should appear in n pairs of opposite vorticity. Moreover, we shall consider in what follows only vortices of the lowest vorticity $q_i{=}\pm 1$, so that $H_\perp$ reads

$$H_\perp = 2n\mu - \pi J \sum_{i\neq j}^{2n} \varepsilon_i \varepsilon_j \ln\frac{r_{ij}}{a}\,, \quad \varepsilon_i = \pm 1\,. \tag{46}$$

The above equation (46) shows the complete analogy between the vortex problem in the XY-model and the problem of the Coulomb gas in two dimensions, where the electrostatic interaction between charges is written as

$$U(r) = -q_0^2 \sum_{i<j}^{2n} \varepsilon_i \varepsilon_j \ln\frac{r_{ij}}{a}\,, \tag{47}$$

where the logarithmic Coulomb interaction arises from solving the Poisson equation (35) in strictly 2D, as we mentioned before. This also means that to preserve the correct dimension of $U(r)$ one should assume that the fictitious charge q_0 in Eq. (47) has dimensions of $(\textit{Energy})^{1/2}$.

This is also consistent with the comparison between Eq. (46) and (47), that allows one to identify the effective charge of the XY-model as

$$q_0^2 = 2\pi J, \tag{48}$$

an equivalence that will be useful below. It is worth discussing what is the physical effect behind the BKT transition within the context of the mapping into the Coulomb-gas problem. As we explained before, we expect that in the low-temperature phase vortices can only exist in pairs, and the correlation function display the quasi-long-range order (11) characterized by a power-law decay. The interaction between charges is provided by Eq. (47) and it is unscreened (in the usual language of charged objects). In contrast, in the high-temperature phase the charges are free to move, leading to the usual metallic screening of the potential. As a consequence, within the context of the Coulomb gas the transition occurs between an unscreened (low-temperature) phase and a screened (high-temperature) phase, where long-range 2D Coulomb interactions are suppressed by the existence of free charges, able to move. Such an analogy is sometimes used to discuss the effect of vortices in terms of an effective dielectric function that screens the bare Coulomb interaction, especially within the context of finite-frequency effects [27,22].
Eq. (46) describes the interaction between vortices in a given configuration with n vortex pairs. In the partition function of the system we must consider all the possible values of n, taking into account that interchanging the n vortices with same vorticity gives the same configuration (so one should divide by a factor $1/(n!)^2$). In conclusion Z reads (up to an irrelevant multiplicative factor Z_{SW} accounting for the partition function of spin-wave excitations connected to the term $H_{\parallel}$ in the Hamiltonian)

$$Z = \sum_{n=1}^{\infty} \frac{1}{(n!)^2} \int d\mathbf{r}_1 \cdots d\mathbf{r}_{2n} e^{-\beta 2n\mu} e^{\pi\beta J \sum\limits_{i\neq j}^{2n} \varepsilon_i \varepsilon_j \ln \frac{r_{ij}}{a}} = \sum_{n=1}^{\infty} \frac{y^{2n}}{(n!)^2} \int d\mathbf{r}_1 \cdots d\mathbf{r}_{2n} e^{2\pi\beta J \sum_{i<j}^{2n} \varepsilon_i \varepsilon_j \ln \frac{r_{ij}}{a}} \tag{49}$$

where we introduced the vortex fugacity

$$y = e^{-\beta\mu}. \tag{50}$$

The explicit derivation of the partition function (49) has the great advantage to introduce one further formal mapping between the original XY-model and a completely different physical problem, that still belongs to the BKT universality class: the quantum sine-Gordon model, defined by the Hamiltonian:

$$H_{sg} = \frac{v_s}{2\pi} \int_0^L dx \Big(K \big(\partial_x \theta\big)^2 + \frac{1}{K} \big(\partial_x \phi\big)^2 - \frac{2g}{a^2} \cos(2\phi) \Big), \tag{51}$$

where θ and $\partial_x \phi$ represent two canonically conjugated variables for a 1D chain of length L, with $\big[\theta(x'), \partial_x \phi(x)\big] = i\pi\delta(x'-x)$, K is the Luttinger-liquid (LL) parameter, v_s the velocity of 1D fermions, and g is the strength of the sine-Gordon potential [18]. In this formulation, the role of the spin angle or phase is played by the field θ. Indeed, when the coupling $g_u = 0$ one can integrate out the dual field ϕ to get the action

$$S_0 = \frac{K}{2\pi} \int dx\, d\tau \left(\big(\partial_x \theta\big)^2 + \big(\partial_\tau \theta\big)^2 \right), \tag{52}$$

equivalent to the gradient expansion (2) of the model (1), once considered that the rescaled time $\tau \to v_s\tau$ plays the role of the second (classical) dimension. The dual field ϕ describes instead the transverse vortex-like excitations. This can be easily understood by considering the quantum nature of the operators within the usual language of the sine-Gordon model. Indeed, a vortex configuration requires that $\oint \nabla\theta \cdot \vec{d\ell} = \pm 2\pi$ over a closed loop, see Eq. (22) above. Since ϕ is the dual field of the phase θ, a 2π kink in the field θ is generated by the operator $e^{i2\phi}$, [18] i.e., by the sine-Gordon potential in the Hamiltonian (51). More formally, one can show that the partition function of the ϕ field in the sine-Gordon model corresponds to the (49) derived above. To see this, let us first of all integrate out the θ field in Eq. (51), to obtain

$$S_{SG} = \frac{1}{2\pi K}\int d\mathbf{r}\big(\nabla\phi\big)^2 - \frac{g}{\pi}\int d\mathbf{r}\cos(2\phi). \tag{53}$$

The overall factor $Z_\parallel = \Pi_{q>0}\big(1/\beta J\mathbf{q}^2\big)$ due to the integration of the θ field (corresponding to the longitudinal excitations $Z_\parallel = \int \mathcal{D}\theta_\parallel e^{-\beta H_\parallel}$ in Eq. (28) above) will be omitted in what follows. We can treat the first term of the above action as the free part

$$S_0 = \frac{1}{2\pi K}\int d\mathbf{r}\big(\nabla\phi\big)^2, \tag{54}$$

and expand the exponential of the interacting part in series of powers, so that

$$Z = \int \mathcal{D}\phi\, e^{-S_0}\sum_{p=0}^{\infty}\frac{1}{p!}d\mathbf{r}_1\cdots d\mathbf{r}_p\left(\frac{g}{\pi}\right)^p\cos\big(2\phi(\mathbf{r}_1)\big)\cdots\cos\big(2\phi(\mathbf{r}_p)\big). \tag{55}$$

Here $\int\mathcal{D}\phi$ is the functional integral over the ϕ field. When we decompose each cosine term as

$$\cos\big(2\phi(\mathbf{r}_i)\big) = \frac{e^{i\phi(\mathbf{r}_i)} + e^{-i\phi(\mathbf{r}_i)}}{2} = \sum_{\epsilon=\pm1}\frac{e^{i\epsilon\phi(\mathbf{r}_i)}}{2}, \tag{56}$$

we recognize that in Eq. (55) we are left with the calculation of average value of exponential functions over the Gaussian weight S_0, i.e of factors

$$\left\langle e^{2i\sum_i \epsilon_i\phi(\mathbf{r}_i)}\right\rangle = e^{2K\sum_{i<j}\varepsilon_i\varepsilon_j \ln\frac{r_{ij}}{a}}\,. \tag{57}$$

Here we followed the analogous steps leading to Eq. (11) above, by recognizing that the above expectation value computed over the Gaussian model (54) is non zero only for neutral configurations $\sum_{i=1}^p \varepsilon_i = 0$, in full analogy with the result found above for the vortices. We then put again $p = 2n$. Taking for instance $\varepsilon_1, \dots \varepsilon_n = +1$ while $\varepsilon_{n+1}, \dots \varepsilon_{2n} = -1$ the combinatorial prefactor $1/p! \equiv 1/(2n)!$ in Eq. (55) should be multiplied times the number $\binom{2n}{n} = (2n)!/(n!)^2$ of possibilities to choose the n positive ε_i values over the $2n$ ones. Thus, Eq. (55) reduces to

$$Z = \sum_{n=1}^{\infty}\frac{1}{(n!)^2}\left(\frac{g}{2\pi}\right)^{2n}\int d\mathbf{r}_1\cdots d\mathbf{r}_{2n}\, e^{2K\sum_{i<j}^{2n}\varepsilon_i\varepsilon_j\ln\frac{r_{ij}}{a}}\,. \tag{58}$$

By comparing Eq. (49) and Eq. (58) we see that the vortex problem (as well as the Coulomb-gas problem) is fully mapped into the sine-Gordon model, provided that we identify

$$K = \frac{\pi J}{T} \quad \text{and} \quad g = 2\pi e^{-\beta\mu}\,. \tag{59}$$

Once more, we have shown that the partition function (58) bears the same structure of the partition function of the interacting system of vortices, or the interacting 2D Coulomb gas. The same equation corresponds however to different physical problems: within the 1D case, we are dealing with a *quantum* phase transition in $1{+}1$ dimension, that describes how the properties of the one-dimensional Luttinger liquid get modified by the interaction term controlled by g. In general, when g increases the ϕ field tends to get trapped in one of the minima of the $\cos(\phi)$ term, and the field becomes "massive". As a consequence, the correlation function of the Luttinger liquid lose the power-law decay characteristic of the "massless" phase, and the system typically describes a (spin or charge) ordered state. Further details on the physical aspects of the 1D analogy are discussed in Ref. [18].
As it is clear from the above derivation, within the XY-model there exists a precise relation (45) between the value of the vortex-core energy μ and the value of the superfluid coupling J. This is somehow a natural consequence of the fact that the XY-model (1) has only *one* coupling constant, J. Thus, when deriving the mapping on the continuum Coulomb-gas problem (46), μ is fixed by the short length-scale interaction, that determines the behavior of $G(r)$ in Eq. (43) and consequently the vortex-core energy (45). In contrast, within the sine-Gordon language μ is determined by the value of the interaction g for the model (53), that can attain in principle arbitrary values. This aspect will be relevant later-on when we discuss the *non-universal* properties of the BKT transition observed in real systems, that do not necessarily follow the same expectations of the XY-model, which is only one of the possible models admitting a BKT transition.

4 BKT physics in superfluids and superconductors

Before discussing the renormalization-group (RG) equations for the BKT model, I will first clarify why BKT physics should be relevant for the superfluid to metal transition in 2D. To understand it, one can start from the very basic consideration [24, 25] that a superconductor develops below T_c a complex order parameter $\psi = \Delta_0 e^{i\theta_0}$, whose amplitude Δ_0 is connected to the SC gap appearing in the quasiparticle spectrum $E_{\mathbf{k}} = \sqrt{\xi_{\mathbf{k}}^2 + \Delta_0^2}$, where $\xi_{\mathbf{k}}$ is the excitation energy above the Fermi level. Below T_c then two possible collective fluctuations [28] of the order parameter are possible, related either to its amplitude Δ or to its phase θ

$$\psi(\mathbf{r}) = \big(\Delta_0 + \Delta(\mathbf{r})\big)e^{i(\theta_0+\theta(\mathbf{r}))}. \tag{60}$$

In analogy with the assumption made before for the XY-model that the modulus of the spins is fixed, under certain circumstances we can assume that the amplitude fluctuations are frozen, and only the phase of the order parameter fluctuates. In this view (that intrinsically assume some form of "preformed" pairing above T_{BKT}, as we shall discuss below) the phase fluctuations are described at Gaussian level by a kinetic-energy term completely analogous to Eq. (2) above. The simplest way to understand this is to start from the order parameter (60) and interpret it as a collective electronic wave function. Within the standard Ginzburg-Landau description of the SC transition [28] one directly expresses the current density in the form analogous to the particle current in first quantization

$$\mathbf{j} = \frac{\hbar q}{2m^*}\Big(-i\psi^*\nabla\psi + i\psi\nabla\psi^*\Big) - \frac{q^2|\psi|^2}{m^*c}\mathbf{A} = \frac{q|\psi|^2}{m^*}\Big(\hbar\nabla\theta - \frac{q}{c}\mathbf{A}\Big) \tag{61}$$

where $\mathbf{A}$ is the gauge potential. As usual, in the absence of phase fluctuations ($\nabla\theta = 0$) one recovers the standard diamagnetic response of the superconductor, as given by the London equation [25]

$$\mathbf{j} = -\frac{e^2 n_s}{mc}\mathbf{A} = -\frac{c}{4\pi\lambda^2}\mathbf{A}, \tag{62}$$

where n_s is the superfluid density, m the electronic mass and λ the penetration depth. As it is well known [25,28], the value of the charge $q = -2e$ in Eq. (61) is fixed by the flux quantization, and it physically represents the fact that the SC order parameter is formed by a Cooper pair. The ratio $|\psi|^2/m^*$ is then equivalent to the combination $n_s/4m$ in the London equation (62). One usually defines $m^* = 2m$ and $|\psi|^2| \equiv n_s/2$ so that Eq. (61) reads

$$\mathbf{j} = -\frac{en_s}{2mc}\left(\hbar\nabla\theta + \frac{2e}{c}\mathbf{A}\right) \equiv -en_s\mathbf{v}_s, \tag{63}$$

with $\mathbf{v}_s$ superfluid velocity. Once established, the relation (63) between the superfluid current and the phase gradient, one can write down the kinetic energy of superfluid electrons in 2D at $\mathbf{A} = 0$ as

$$H_s = \frac{1}{2}mn_s^{2d}\int d\mathbf{r}\, v_s^2(\mathbf{r}) = \frac{\hbar^2 n_s^{2d}}{8m}\int d\mathbf{r}\big(\nabla\theta\big)^2, \tag{64}$$

where we made explicit the emergence of a 2D superfluid electron density n_s^{2d} such that the quantity $\hbar^2 n_s^{2d}/m$ has the dimension of an energy. By direct comparison between Eq. (64) and Eq. (2) we understand that Gaussian fluctuations of the SC phase of the order parameter are described by the same model obtained by a low-energy approximation to the XY-model. In this case, the role of the coupling J of the XY-model is played by the energy scale connected to the superfluid density in 2D. To make a further connection to the physically-measured penetration depth λ, appearing in the London equation (62), we must convert the 3D superfluid density n_s given in Eq. (62) to an effective 2D one, by using a transverse dimension d. This can represent the film thickness in a thin film, or the distance between planes in weakly coupled layered superconductors (as it is the case for cuprate superconductors). We can then identify the so-called superfluid rigidity or stiffness as the energy scale set by the superfluid density in 2D

$$J = \frac{\hbar^2 n_s^{2d}}{4m} = \frac{\hbar^2 c^2 d}{16\pi e^2\lambda^2}. \tag{65}$$

To get an idea of the energy scales, it can be useful to express J in Kelvin: since usually the penetration depth is given in microns, one obtains

$$J = 0.62 \times \frac{d[\text{Å}]}{\lambda^2[\mu\text{m}^2]}[K] \tag{66}$$

Typical values [25] of the penetration depth at $T{=}0$ can range from around $\lambda(T{=}0) \sim 0.045$ µm in conventional BCS superconductors, like Al, to $\lambda(T{=}0) \sim 0.16$ µm in cuprate superconductors. As a consequence, if one computes the stiffness per plane in a typical cuprate system, putting the inter-plane distance at $d \sim 5$ Å in Eq. (65), one gets a stiffness of the order of $J_s \sim 120$ K, i.e., not far from the critical temperature of these materials, and much smaller than the pseudogap scale measured above T_c (that can be as large as 20–30 meV). Such an observation motivated, in a milestone paper in the middle 90ties, the proposal that phase fluctuations (and eventually BKT physics) could be relevant for this class of materials [29]. However, as we shall discuss below, the expectation that a layered superconductor with weakly-coupled planes should behave as a quasi-2D system is not always obviously realized, and nowadays convincing evidence of the occurrence of a BKT transition in *bulk* layered cuprates is still lacking.

It is worth stressing that the Gaussian phase-only model (64), that we discussed within a classical Ginzburg-Landau picture, can be derived by starting from a microscopic BCS model by integrating our the fermionic degrees of freedom, as discussed, e.g., in Ref. [24, 30] and references therein. More specifically, one can show in full generality that in the SC state the coefficient of the $\left(\nabla\theta\right)^2$ term in the effective phase-only action is given by the physical superfluid density, defined as the static transverse limit of the current-current correlation function, as it is implicit in the London equation (62). This has also the relevant consequence that J from Eq. (65) should already include the temperature depletion due to *quasiparticle* excitations, not captured by the BKT physics, that only deals with the temperature effects due to proliferation of vortexes. This point will be relevant below while discussing the physical conditions for the observation of BKT physics in effectively 2D superconductors. Indeed, while in 3D the superfluid density is expected to go to zero continuously at the BCS transition T_c, that we will denote in what follows as the mean-field one, within the BKT theory the hallmark of vortex proliferation will be the emergence of a discontinuous jump of the superfluid density at T_{BKT}, as we shall see in the next Section.

Finally, it is crucial to realize that the BKT physics only deals with *classical transverse* phase fluctuations, as it is evident from the phase-only model (64), where no dynamics of the phase degrees of freedom is included. We then expect that such a description can only be valid near T_c, where quantum effects are suppressed and phase fluctuations can be treated as classical. In contrast, as $T \to 0$ one should promote the classical model (64) to a *quantum* one, adding to Eq. (64) the energetic cost to perform a phase gradient *in time* , that is controlled by the charge compressibility κ_0 [24, 31], so that Eq. (64) is replaced at $T = 0$ by the quantum action

$$S = \frac{\hbar^2}{8} \int dt \, d\mathbf{x} \left(\kappa_0 \left(\partial_t \theta\right)^2 - \frac{n_s}{m} \left(\nabla\theta\right)^2 \right). \tag{67}$$

For weakly-interacting *neutral* systems κ_0 in the static long-wavelength limit can be approximated with the density of states at the Fermi level, and by Fourier transforming Eq. (67) one recognizes the so-called [31] Anderson-Bogoliubov sound mode

$$\omega^2 = v_s^2 |\mathbf{k}|^2, \tag{68}$$

where $v_s^2 = n_s/m\kappa_0$ is the sound velocity. The appearance of the charge compressibility as a coefficient of the time gradient in Eq. (67) is a direct consequence of the fact that density and phase are quantum-mechanically conjugate variables [28]. However, in the case of *charged* superconductors this also implies that the charge compressibility at long wavelength is modified, as compared to the neutral case, by he presence of long-range Coulomb interactions, so the term κ_0 in Eq. (67) is replaced in Fourier space by $\kappa(\mathbf{k}) = \kappa_0/\big(1+V(\mathbf{k})\kappa_0\big)$, where $V(\mathbf{k})$ is the Coulomb potential in generic D dimensions. Since for $\mathbf{k} \to 0$ one has $\kappa \to 1/V(\mathbf{k})$ the spectrum of the phase mode, that reflects the one of density fluctuations, identifies now a plasma mode, whose energy vs. momentum dispersion depends on the dimensions. In the standard isotropic three-dimensional (3D) case one recovers [30, 31] the well-known dispersion

$$\omega^2 = \omega_p^2 + v_s^2\,|\mathbf{k}|^2, \tag{69}$$

where $\omega_p^2 = 4\pi e^2 n_s/m$ is the isotropic plasma frequency. The main consequence of the emergence of a gapped plasmon in the phase spectrum is that the longitudinal phase fluctuations, that are the main source of the low-T suppression of the stiffness within the classical XY-model [24, 32] (see also next Section), are converted from the sound-like mode of Eq. (68) to a gapped plasma mode, leading to a thermal suppression of any contribution to the stiffness due to anharmonic phase fluctuations beyond Gaussian level [30], due to the fact that the plasma frequency at zero temperature can be as large as the normal-state one, that is of the order of eV. This is the main reason why the BCS theory, that only accounts for the effects of quasiparticle excitations on the temperature depletion of the superfluid stiffness, successfully describes the temperature dependence of $J_s(T)$ in all 3D superconductors: quantum phase fluctuations beyond Gaussian level barely contribute to deplete the superfluid density, due to the large energetic cost of their thermal excitation. On the other hand, as T approaches T_c the energy scale of Eq. (65) is progressively suppressed by thermal quasiparticle excitations, the phase fluctuations recover a classical behavior, and transverse vortex-like excitations can become relevant in 2D systems. Their effect will then add to the one of quasiparticle excitations, as we will discuss in the next Section.

5 Renormalization-group equations for the BKT transition

I will not derive here the renormalization-group (RG) equations of the BKT model, but I will rather discuss their consequences. Their derivation can be found in the original paper [26] and in various book, like, e.g., in Ref. [18]. On very general grounds, the RG equations represent the result of a coarse-graining procedure: the physical goal is to integrate out the interaction effects at the short scale, in order to capture the long-scale behavior of the system, that is the relevant one in the thermodynamic limit. To fix also the language once and for all, I will discuss the RG results within the context of 2D superconductors, referring then to a transition from a superfluid state, where the superfluid stiffness (65) is finite, to a metallic one, where $n_s^{2d} = 0$ and the system is no more superfluid.

The derivation of the partition function for the Coulomb-gas model (49) and for the sine-Gordon model (58) has shown that in both cases it can be expressed in terms of the two quantities K and g defined in Eq. (59). Within the context of the SC transition, the large-distance behavior of K defines the large-distance behavior of the phase rigidity J, that tells us if the system remains superfluid in the thermodynamic limit [21]: in other words, the physical value of the superfluid density J_s, that is the quantity experimentally accessible, is obtained under RG flow from the limiting value of K as $\ell \to \infty$

$$J_s \equiv \frac{TK(\ell{\to}\infty)}{\pi}\,. \tag{70}$$

On the other hand, the behavior of the vortex-fugacity g at large distances will tell us if vortices proliferate, leading to a growing of g, or remain bound in pairs, that slightly renormalize J_s with respect to the short-scale value J, without suppressing the superfluid behavior. We will use here the two variables from (59), that naturally occur as coupling constant in the sine-Gordon model. We will assume at each temperature as starting values

$$K(\ell{=}0) = \frac{\pi J(T)}{T} \quad \text{and} \quad g(\ell{=}0) = 2\pi e^{-\beta\mu(T)}\,, \tag{71}$$

where $J(T)$ is given by the value of the stiffness including all other thermal effect besides vortex excitations. For example, within the context of superconductors it will be the stiffness (65) at a given temperature, including the thermal suppression due to quasiparticles. For what concerns the vortex-core energy $\mu(T)$ we will always assume a constant ratio $\mu(T)/J(T) = \mathit{const}$, so that $\mu(T)$ also includes thermal effects due to other excitations of the system. Eqs. (71) identify a line in the (K, g) plane where the RG flow starts, as shown in Fig. 1. Using these two variables the RG equations read

$$\frac{dK}{d\ell} = -K^2 g^2 \quad \text{and} \quad \frac{dg}{d\ell} = \big(2{-}K\big)g\,. \tag{72}$$

By direct inspection of Eqs. (72) one sees that there are two main regimes, represented in Fig. 1: for $K \gtrsim 2$ the r.h.s. of Eq. (72) is negative, so that $g \to 0$ and K tends to a finite value $K \to K^*$ that determines the physical stiffness J_s, according to Eq. (70). Instead for $K \lesssim 2$ the vortex fugacity grows under RG flow, K in Eq. (72) scales to zero, and $J_s = 0$. The BKT transition temperature is defined as the highest value of T such that K flows to a finite value. This occurs at the fixed point $K = 2, g = 0$, so that at the transition one always has

$$K(\ell{\to}\infty,\, T_{BKT}) = 2 \quad \Rightarrow \quad \frac{\pi J_s(T_{BKT})}{T_{BKT}} = 2. \tag{73}$$

As soon as the temperature grows above T_{BKT}, $K \to 0$, so also $J_s \to 0$. As a result, one finds $J(T_{BKT}^+) = 0$, i.e., the superfluid density jumps discontinuously to zero right above the transition. The equation (73) describes the so-called universal relation between the transition temperature T_{BKT} and the value of the superfluid stiffness J_s at the transition, and represents a more refined version of the relation (26) based on the balance between the energy and the entropy of a single-vortex configuration.

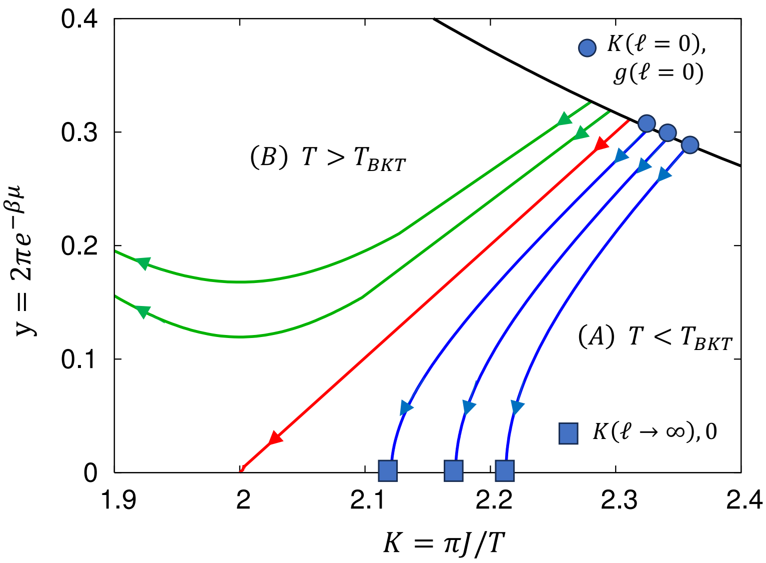

Fig. 1: *RG flow for the BKT problem. The solid black line identifies, for each temperature, the starting values of $K(\ell{=}0)$ and $g(\ell{=}0)$ (denoted with circles) given by Eq. (71). Under the RG flow $K(\ell), g(\ell)$ evolve along the lines shown in blue (for $T{<}T_{BKT}$) and green (for $T{>}T_{BKT}$). For $T{<}T_{BKT}$ the flow at $\ell{\to}\infty$ reaches the point $(K^*, 0) = \big(K(\ell{\to}\infty), 0\big)$, denoted with squares, where vortices disappear and the system has a finite stiffness. At $T{=}T_{BKT}$ the RG equations flow to the fixed point $K{=}2$, $g{=}0$, that allows one to establish the universal relation (73). Above T_{BKT} the flow tends to $(0, \infty)$, so free vortices proliferate and the stiffness goes to zero.*

To better visualize the role of vortex-antivortex pairs it is instructive to derive the temperature dependence of $J_s(T)$ as obtained by numerical solutions of the RG equations. As an example we show in Fig. 2 the expected temperature dependence in the XY-model. As explained above, the BKT RG equations account only for the effect of vortex excitations, so that any other excitation that contributes to the depletion of the superfluid stiffness must be introduced by hand in the initial values of the running couplings. For example, in real superconductors there are also quasiparticle excitations, as we explained above, while in the XY-model there are also longitudinal phase fluctuations, that give rise to a linear depletion to the superfluid stiffness at low temperature $J(T) = J_0\big(1{-}T/4J\big)$ (see e.g. Ref. [32] and references therein). One could then be tempted to use the relation (73) to estimate the T_{BKT} value by looking for the intersection between the universal line $2T/\pi$ and the $J(T)$ expected from the remaining excitations except the vortices. However, such a procedure can only be approximate, since in relation (73) the temperature dependence of $J_s(T)$ is determined also by the presence of bound vortex-antivortex pairs, which can renormalize J_s already *below* T_{BKT}. This effect is connected to the difference between the initial value of $K(0)$ at each temperature, and its asymptotic value $K^* = K(\ell{\to}\infty)$, that determines J_s according to Eq. (70). The crucial observation at this point is that the difference between K and K^* quantitatively depends on the value of μ: as μ decreases the renormalization of J_s due to bound vortex pairs below T_{BKT} increases, the $J_s(T)$ curve starts to deviate from the bare dependence of $J(T)$ (due to other excitations besides vortices) and consequently T_{BKT} is further reduced with respect to the mean-field critical temperature T_c (i.e. the one where $J(T_c){=}0$). As an example we show in Fig. 2 the behavior of $J_s(T)$ using a bare temperature

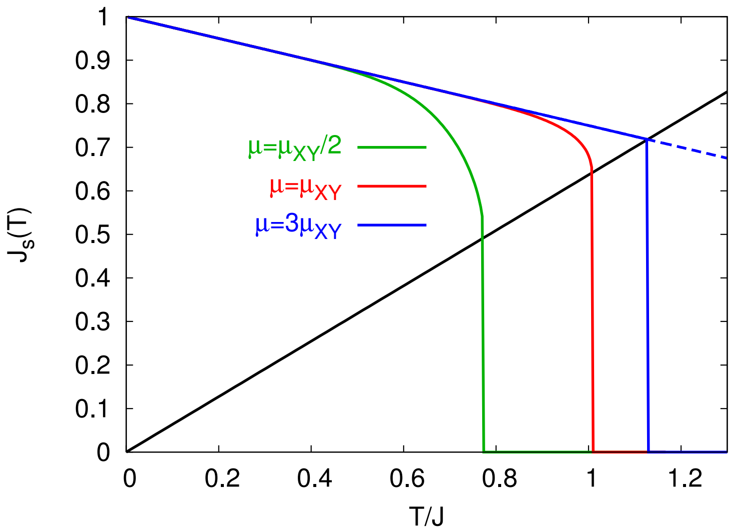

Fig. 2: *Solution of the RG equations by using a linear temperature dependence for $J(T) = J_0(1-T/4)$, with $J_0 = 1$, to mimic the behavior of the bare stiffness within the XY-model. Different curves correspond to different values of the ratio μ/J, measured in units of the value (45) it has within the XY-model. Notice that for small μ values the deviation of $J_s(T)$ from $J(T)$ starts much before than the temperature where the universal jump occurs: this is due to the larger density of vortex-antivortex pair present below T_{BKT}, due to smaller the energetic cost to create them on the shortest length scale.*

dependence as in the XY-model and switching the vortex-core energy from the value (45) to values smaller or larger. As one can see, for decreasing μ the effect of bound vortex-antivortex pairs below T_{BKT} is significantly larger, moving back the transition temperature to smaller values. In the light of this observation, one must be very careful in defining what is universal: T_{BKT} is *not* universal, what is universal in the relation between the *renormalized* superfluid density and the transition temperature, as encoded in Eq. (73).

Finally, it is worth spending still some time on the RG equations (72) to derive the expression of the correlation length ξ close to the BKT critical point. Let us start with a convenient change of variables

$$x = K - 2 \quad \text{and} \quad y = 2g\,, \tag{74}$$

so that the RG equations with this choice read

$$\frac{dx}{d\ell} = -(x+2)^2 \frac{y^2}{4} \simeq -y^2, \tag{75}$$

$$\frac{dy}{d\ell} = -xy, \tag{76}$$

where we approximated the first RG equation around the fixed point $x = 0$, $y = 0$. We can easily solve these differential equations by noticing that they can be rewritten as

$$x\frac{dx}{d\ell} - y\frac{dy}{d\ell} = 0, \tag{77}$$

whence

$$x^2 - y^2 = A^2. \tag{78}$$

Eq. (78) is nothing but the RG flow, close to the fixed point $(x, y)=(0, 0)$, in the new x-y plane. The resulting flow lines are hyperbolas, whose symmetry axis can be: $y = 0$ if $A^2 > 0$ (equivalent to the green lines in the region (B) of Fig. 1) or $x = 0$ if $A^2 < 0$ (region (A) of Fig. 1). The critical line corresponds obviously to $A^2 = 0$.
Approaching the critical point $A \to 0^+$, Eq. (75), can be rewriten as

$$\frac{dx}{d\ell} = -x^2, \tag{79}$$

whose solution is

$$x = \frac{1}{\ell + c}, \tag{80}$$

where c is a constant connected with the initial value of the RG flow $\ell = 0$ and $x(0)$. Along the critical line x will finally flow to zero but in an extremely slow fashion, i.e., with the log of the rescaled lattice spacing $\ell = \ln(a'/a)$. Analogously we find in the regime $A^2 > 0$ that x (and then K) flows to a finite value: it then corresponds the low-temperature region, having a finite superfluid stiffness and vanishing g. Indeed, by substituting $x^2 = y^2+A^2$ in (76), we get a first-order differential equation for y

$$\frac{dy}{d\ell} = -y\sqrt{y^2 + A^2}, \tag{81}$$

whose solution is

$$y(\ell) = \frac{A}{\sinh\big(A\ell + \operatorname{arcsinh}(A/y_0)\big)} \xrightarrow[\ell\to\infty]{} 0. \tag{82}$$

On the other hand, following the same procedure, the solution for x will be

$$x(\ell) = \frac{A}{\tanh\big(A\ell + \operatorname{arcsinh}(A/y_0)\big)} \xrightarrow[\ell\to\infty]{} A. \tag{83}$$

Hence, as expected the superfluid stiffness tends to a finite value, while the coupling accounting for the vortices vanishes under coarse graining.
The opposite regime, the one where $A^2 < 0$, corresponds to the region $T > T_{BKT}$. Here the superfluid stiffness goes to zero, and we can definite the correlation length as the scale where this happens. In other words, the correlation length can then be estimated as the scale ℓ^* at which $x(\ell^*) = 0$. For simplicity let us introduce another constant C, such that: $-A^2 = C^2 > 0$. After having expressed $y^2 = x^2 + C^2$, we can solve the differential equation (75):

$$\frac{dx}{d\ell} = -\big(x^2+C^2\big) \implies \frac{x}{C} = \tan\big(-C\ell + \arctan(x_0/C)\big). \tag{84}$$

From (84), we then have that x vanishes at the scale

$$\arctan\frac{x}{C} = c\ell^*. \tag{85}$$

Near the transition, we also know that $x_0 \sim y_0$, hence: $C^2 = y_0^2-x_0^2 = (y_0-x_0)(y_0+x_0) \simeq 2y_0(y_0-x_0)$. Since at the transition is $x=y$, the difference between the initial values y_0-x_0 is at leading order proportional to the distance from the transition temperature, i.e. $(y_0-x_0) \propto (T-T_{BKT})/T_{BKT}$. Thus we obtain

$$C = \alpha\sqrt{t}, \tag{86}$$

where α is a constant of order one and t is the reduced critical temperature

$$t = \frac{T - T_{BKT}}{T_{BKT}}. \tag{87}$$

Finally, since we are working in the limit $t \ll 1 \to \arctan(x_0/C) \simeq \pi/2$, from Eq. (84) we derive that

$$C\ell^* \sim O(1) \implies \ell^* = \frac{b}{\sqrt{t}}. \tag{88}$$

Since $\ell^* = \ln(\xi/a)$, we have that

$$\xi/a = e^{b/\sqrt{t}}. \tag{89}$$

The parameter b in Eq. (89) depends on the specific model studied. Eq. (89) shows one of the most prominent hallmarks of the BKT transition: by approaching the critical temperature from above the correlation length displays an exponential divergence in the reduced critical temperature t, instead of the usual power-law divergence observed in ordinary Ginzburg-Landau transition, see Eq. (15) above.

6 Superfluid density in thin films of superconductors

In the previous Section we identified at least two typical signatures of BKT physics that are significantly different from the analogous expectations for 3D superconductors: the discontinuous and universal jump (73) of the superfluid stiffness J_s at T_{BKT}, to be contrasted with the continuous suppression of J_s at the critical temperature T_c in 3D, and the exponential activation (89) of the correlation length as T_{BKT} is approached from above. Let us first discuss under which conditions the universal jump of J_s has been measured in real systems, where additional effects not discussed so far very often make such a jump rather elusive.

The first experimental observation of the universal jump (73) has been actually done in thin films of superfluid helium [4, 5]. An example is shown in Fig. 3. Here the experimentally accessible quantity is the shift of the rotation period $\varDelta P(T)$ of a torsion pendulum immersed in liquid helium. The rotation period depends on the inertia momentum of the pendulum, that changes below T_{BKT} due to the fact that it cannot drag anymore with it the superfluid fraction of the liquid. As a consequence $\varDelta P(T) \propto J_s(T)$, so that the $\varDelta P$ jump corresponds to the jump (73) of the superfluid stiffness due to the free-vortices proliferation. As one can see, regardless of the $T = 0$ value of J_s the jump always occurs when $J_s(T)$ intersects the BKT line $2T/\pi$: thus, as evidenced above, T_{BKT} is not by itself universal, but the universal relation (73) is always satisfied.

As mentioned at the beginning, in the original paper by Kosterlitz and Thouless [2] it was questioned the possibility to realize a BKT transition in SC films. The objection arises from the fact that in a *charged* superfluid, as is the case for superconductors, a vortex carries a supercurrent,

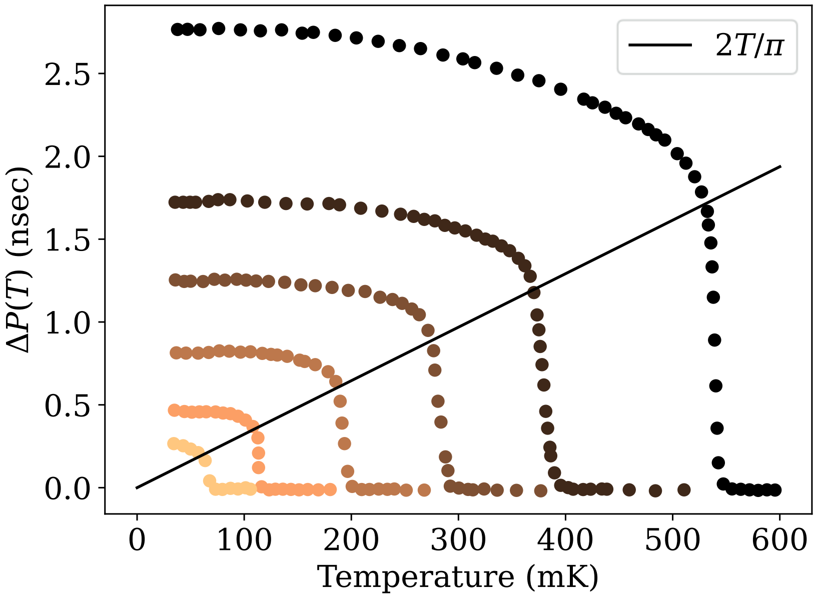

Fig. 3: *Superfluid-density measurements via the oscillator period shift $\Delta P(T)$ of a torsion pendulum for different films of pure ^{4}He. Each curve corresponds to a different value of the thickness d, such that $\Delta P(T{=}0)$ decreases with decreasing d. The intersection with the solid line $2T/\pi$ represent the T_{BKT} temperature as defined by the universal-jump relation* (73). *The experimental data have been taken from Ref. [5].*

that contributes itself to the interaction between vortices. In the usual 3D case this mechanism cut-offs the interaction between vortices at a scale λ fixed by the penetration depth [25], leading to a failure of the long-distance $\log$ interaction between vortices that is at the heart of the interacting Hamiltonian (46). However, a crucial observation [33, 22] in this respect is that when the SC system becomes a *thin* film, the interaction between vortices is screened by the supercurrents at a much larger distance $\Lambda = \lambda^2/d$, set by the film thickness d itself, the so-called Pearl length from the name of the scientist who discussed this issue for the first time [34]. An additional effect is that when the film thickness decreases also the relative effects of disorder increase, contributing to a significant increase of λ due to the paramagnetic suppression of the superfluid density [25]. This implies that in practice, for sufficiently thin films with large disorder, where λ is very large, and for temperatures near the mean-field critical temperature T_c, where J is further suppressed by thermal quasiparticle excitations, the electromagnetic screening effects come in at a scale Λ even larger than the system size, making the occurrence of a BKT transition possible. It is worth noting that, on very general grounds, this discussion implies that the BKT transition in charged superconductors is possible whenever d is very small or λ is very large. From the relation (65) it follows that whatever mechanism suppresses n_s^{2d}/m it also leads to a large λ, allowing one for a description of the vortex interaction as the one expected in a neutral superfluid. While in thin films of conventional superconductors [10] this usually happens as an effect of disorder on n_s^{2d}, in unconventional superconductors like the cuprates this suppression is observed by proximity to a Mott phase, loosely speaking as an effect of mass-renormalization enhancement [29]. In other words, systems with low intrinsic superfluid rigidity are better candidates for the observation of BKT physics, since screening effects are

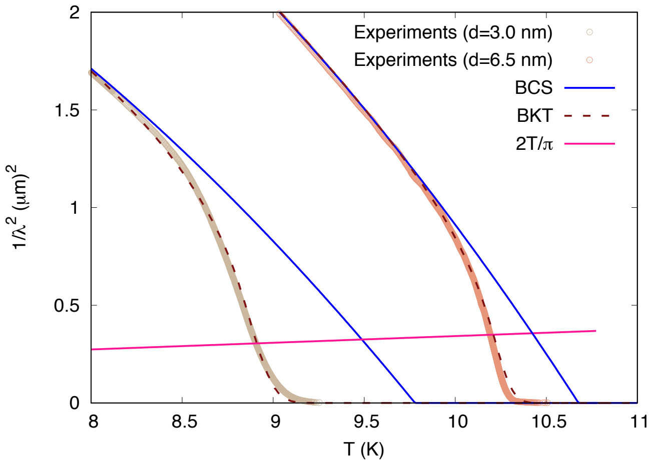

Fig. 4: *Measured temperature dependence of the superfluid density in thin NbN films with different thickness. Data are taken from Ref. [10], along with the BCS fit and the theoretical BKT fit, obtained by using $\mu/J = 1.19$ for $d = 3$ nm and $\mu/J = 0.61$ for $d = 6.5$ nm. Notice that the jump here is further smeared out by the inhomogeneity.*

relevant only above a very large Pearl length Λ. In addition, as we commented already before in relation to Eq. (66), a low stiffness implies an energy scale for J_s comparable to the mean-field T_c, making in practice the intervale T_c–T_{BKT} *larger*. To understand this, we should consider that within BCS theory [25] the temperature-dependent bare stiffness $J(T)$ which enters the BKT RG equations vanishes near T_c in a Ginzburg-Landau fashion [28] as

$$J(T) \simeq J_0 \left(1 - \frac{T}{T_c}\right), \tag{90}$$

where

$$J_0 \sim \gamma J(T{=}0), \tag{91}$$

and γ is a constant of order 1. As a consequence, an order-of-magnitude estimate of the T_{BKT} temperature obtained by the universal relation (73) is

$$J_0 \left(1 - \frac{T}{T_c}\right) = \frac{2}{\pi} T_{BKT} \quad \Rightarrow \quad \frac{T_c - T_{BKT}}{T_c} = \frac{1}{1 + \frac{\pi}{2}\frac{J_0}{T_c}}\,. \tag{92}$$

One then understands that as J_0/T_c decreases, as it happens when the film thickness decreases or the superfluid fraction is suppressed by disorder and/or correlations, the distance between T_c and T_{BKT} increases, making it easier to discriminate the two in experiments. In this view, the mean-field temperature T_c can be interpreted as the temperature where pairing forms, so that the amplitude fluctuations can be neglected at $T < T_c$ and one goes back to an effective phase-only model as the one assumed within the BKT approach. In this sense the BKT physics implies a "preformed pairing" in a rather small temperature range, i.e., between T_c and T_{BKT}.
The first observations of BKT physics in thin films of SC date back to the late 80's. However, they were not based on the direct measurement of J_s, but rather to its indirect estimate via I-V characteristics [8, 9], that we will discuss below. This is due to the fact that only in the

late nineties emerged an experimental technique able to measure the penetration depth of thin films via the so-called two-coil mutual inductance technique [35] (an experimental technique triggered, as many others, mostly by the investigation of high-temperature cuprate superconductors). Fig. 4 shows one example of λ^{-2} measured in thin films of NbN, a conventional s-wave superconductors, taken from Ref. [10]. As established in Eq. (65) above, this is directly proportional to the superfluid stiffness $J_s(T)$ of the system. Here one can recognize two different theoretical curves: the fit of the low-temperature part $J_{BCS}(T)$, which is based on a standard BCS-like suppression of $J_s(T)$, present also in 3D samples, and the BKT fit, that reproduces the experimental observations, along with the universal $2T/\pi$ line, rescaled to get an inverse length squared. As one can see, $J_s(T)$ displays a rapid downturn around the intersection with the $2T/\pi$ line, but this is not the sharp jump predicted by Eq. (73). This experimental finding has been interpreted [10] as an effect of sample *inhomogeneity*, that one can phenomenologically model as a finite probability P_i of having a range of possible $J_s^i(0)$ values, leading to different T_{BKT}^i temperatures. The measured $J_s(T)$ appears then as an average of the different $J_s^i(T)$ realizations: since, according to Eq. (92), smaller $J_s^i(0)$ lead to smaller T_{BKT}^i, the averaged $J_s(T)$ will display a smeared jump, as observed experimentally. Even though the concept of inhomogeneity has been introduced at the beginning as phenomenological, more recently [36] we worked on a theoretical validation of it based on Monte Carlo simulations on a disordered version of the XY-model (1)

$$H_{XY} = -\sum_{\langle ij\rangle} J_{ij}\cos\big(\theta_i - \theta_j\big), \tag{93}$$

where the local couplings J_{ij} have a finite randomness around an average value $\bar{J}_{ij}$ that sets the scale of the transition. The main point is that in principle one would expect that the universal jump (73) is insensitive to the presence of randomness on the J_{ij} coupling. The reason relies on the so-called Harris criterium [37], which establishes under which condition finite-size effects due to disorder are more relevant that the finite size L of the system itself. This estimate can be done by considering that T_c can still be well identified if the temperature indetermination $|T - T_c|$ itself is larger that the T_c indetermination ΔT_c due to disorder, i.e. $|T - T_c| \gg \Delta T_c$ as $T \to T_c$. In D dimensions one can estimate ΔT_c by the following argument: let us assume that the system is ordered on a typical scale of size ξ, the correlation length of the pure system, and let us estimate the variance of the local values of T_c in the disorder system via the central theorem, stating that it scales with the square root of the N possible values of the variable itself, that in turn scales with the volume ξ^D. Thus we could say that

$$\Delta T_c \sim \frac{1}{\sqrt{\xi^D(T)}} = \frac{1}{\xi^{D/2}(T)}\,. \tag{94}$$

If we plug into Eq. (94) the usual power-law scaling of $\xi(T)$ from Eq. (15) we obtain that disorder-induced uncertainty in the transition is irrelevant when

$$|t| \gg 1/|t|^{\nu D/2} \quad\Rightarrow\quad \nu > 2/D\,, \tag{95}$$

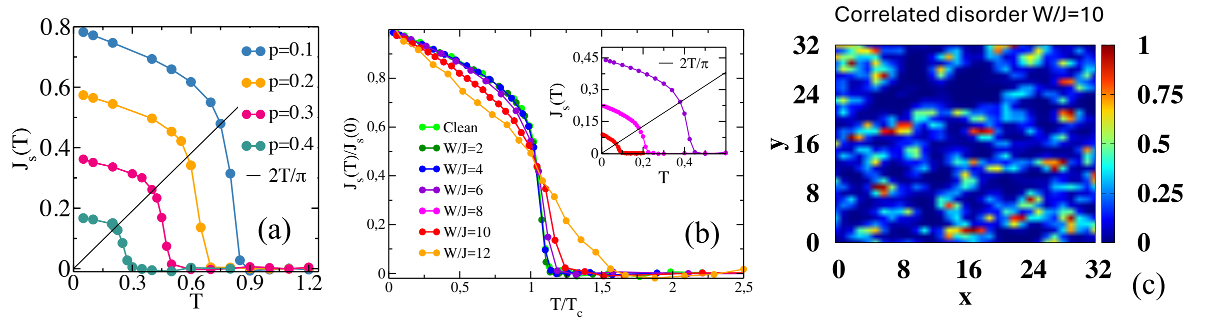

Fig. 5: *Monte Carlo simulations on the disordered XY-model (93) for different types of disorder, implemented via the space structure of the local couplings J_{ij}. (a) Diluted XY-model. In this case $P(J_{ij}) = 1$ with probability p. As one can see, as disorder increases the $J_s(T{=}0)$ is suppressed, along with T_{BKT}, but the universal relation (73) is always observed. Figure adapted from Ref. [32]. (b) Correlated disorder, as generated via a quantum XY-model in random transverse field. A typical map of the local coupling at the disorder level $W/J = 10$ is shown in panel (c). More details on the generation of the maps of local couplings can be found in Ref. [36]. In this case as the disorder strength W/J increases not only the overall scale of the stiffness is suppressed (see inset), but the universal jump is progressively smeared out by disorder. Figures adapted from Ref. [36]*

with $t = (T - T_c)/T_c$. The reasoning is that under the condition (95) weak disorder decreases under coarse graining and becomes unimportant on large length scales, making the clean critical point stable against weak disorder. As we have seen before, in the BKT transition the correlation length $\xi(T)$ diverges *exponentially* as $T \to T_{BKT}$, which means that $\nu = \infty$ within the context of the Harris criterium (the exponential is faster than any power law). One would then conclude that the Harris criterium (95) is always satisfied for BKT physics, disorder is always irrelevant, and the BKT jump (73) should be robust against disorder. Such a result holds indeed for *uncorrelated short-range* disorder, as it is shown in Fig. (5)a, where we show results for a disordered XY-mode with link dilution [36]. However, when disorder is *correlated*, as it happens, e.g., when the local coupling constants J_{ij} have a “granular” structure, see Fig. 5c, the Harris criterium does not hold and one could expect modifications of the BKT jump. Such an effect has been proved by means of Monte Carlo simulations in Ref. [36]: here it has been shown that when the J_{ij} couplings realize a fragmented SC state the BKT jump is symmetrically smeared out with respect to the expected transition, see Fig. 5b, in strong analogy with the experimental observations in thin SC films as the one reported in Fig. 4. This result has been explained in terms of an unconventional vortex-pairs nucleation in the granular SC state. Indeed, the presence of large regions with low couplings J_{ij} allows the system to nucleate several vortex-antivortex pairs already well below T_{BKT}, leading to a continuous downturn of the $J_s(T)$ instead of the expected jump.

A second aspect relevant for the understanding of the BKT transition in real materials is the role played by the vortex-core energy. Indeed, apart from the smearing of the jump, the measured $J_s(T)$ appears to deviate from the BCS behavior significantly before the intersection with the BKT line $2T/\pi$. As we discussed within the context of Fig. 2, this is an effect of the vortex-antivortex pair renormalization of the stiffness that occurs already below T_{BKT}, and it depends on the value of the vortex-core energy. Within the XY-model (1) there exists a single energy scale, J, so that, when we mapped it into the continuum Coulomb-gas problem, the ratio μ/J simply followed from the regularization of the function $G(r)$ at the length scale a of the original lattice model, see Eqs. (42), (43) and (45). However, in a BCS superconductor one would rather fix the value of the vortex-core energy by computing exactly the energy per unit-length of a vortex line [25]

$$I = \left(\frac{\Phi_0}{4\pi\lambda}\right)^2 \left(\log\frac{\lambda}{\xi_0} + \epsilon\right) \equiv \pi J \left(\log\frac{\lambda}{\xi_0} + \epsilon\right)$$

so that according to our definition $\mu = \pi\epsilon J$. A precise estimate of $\epsilon \simeq 0.497$ for the vortex core in three-dimensional geometry is given in Refs. [38, 39], so that within BCS theory one could eventually expect values of μ significantly smaller than within the XY-model,

$$\mu_{BCS} \simeq \pi J/2 \simeq \mu_{XY}/\pi. \tag{96}$$

A similar result can be obtained by using a different argument, i.e., by estimating μ from the condensation energy lost in creating the vortex core [10]. In this case one would put

$$\mu_{BCS} = \pi\xi_0^2\varepsilon_{cond}, \tag{97}$$

where ε_{cond} is the condensation-energy density. In the clean case Eq. (97) can be expressed in terms of J_s by means of the BCS relations for ε_{cond} and ξ_0. Indeed, since $\varepsilon_{cond} = dN(0)\Delta^2/2$, where $N(0)$ is the density of states at the Fermi level, Δ is the BCS gap, and ξ_0=ξ_{BCS}=$\hbar v_F/\pi\Delta$, where v_F is the Fermi velocity, assuming that n_s=n at T=0, where n=$2N(0)v_F^2 m/3$, one has

$$\mu_{BCS} = \frac{\pi\hbar^2 n_s d}{4m}\frac{3}{\pi^2} = \pi J_s\frac{3}{\pi^2} \simeq 0.95 J_s\,, \tag{98}$$

that is again of the same order of magnitude of Eq. (96) above. Interestingly, in Ref. [10] it was observed that as the film thickness decreases, the ratio μ/J_s extracted from the fitting of the $J_s(T)$ curve increases. This effect can be understood within a model for disordered superconductors, resulting from an increasing separation between the energy scales associated with the gap and the stiffness, that emerged as a signature of the superconductor-to-insulator transition induced by disorder [40].

The possibility of observing BKT jumps has been discussed in a wide variety of thin films of superconductors: besides the conventional NbN mentioned above, one could list InO_x films, cuprate superconductors, but also the 2D electron gas formed at the interface between artificial heterostructures made of insulating oxides as $LaAlO_3$/$SrTiO_3$, $LaTiO_3$/$SrTiO_3$ [14,15] and more recently even Al/$KTiO_3$ interfaces [16]. A review of these systems and some relevant references can be found in [20]. A related but slightly different issue is instead the observation of BKT physics in *bulk* cuprate superconductors. In this case, one is dealing with a full 3D system, but with weakly coupled SC layers. As we mentioned before, one could argue [29] that each unit behaves as a 2D superconductor, with a characteristic effective thickness d corresponding to the interlayer distance, with the interlayer coupling leading simply to a rounding of the BKT jump. However, as we discussed in Ref. [19], this expectation is only partly realized, and actually the effective BKT temperature of a layered 3D system can move considerably away from the BKT temperature of each isolated unit as the vortex-core energy increases.

7 Signature of BKT physics in other experimental quantities

7.1 I-V characteristics

As mentioned in the previous Section, direct measurements of the universal jump (73) of the superfluid density were possible only from the middle nineties. Nonetheless, Halperin and Nelson in their milestone paper on the applicability of BKT physics to superconductors [22] proposed to access indirectly the J_s jump via a measurement of the I-V characteristics below T_{BKT}. The basic idea is that below T_{BKT} the vortices are bound in pairs: however, a large enough applied current can unbind a certain fraction of vortices, leading to a power-law dependence of V on I that is controlled by the superfluid stiffness. To understand how these two quantities are related, let us consider a film of length L along x and width W along y, and let us consider a finite current I along x, corresponding to a current density $\mathbf{j} = I/(Wd)\hat{x}$. This current produces a force (Magnus force or Lorentz force) per unit length of the vortex line that moves vortices perpendicularly with respect to $\mathbf{j}$, with a direction determined by the sign of the vorticity ε_i=± 1

$$\mathbf{f} = \varepsilon_i \, \mathbf{j}_s \times \hat{z} \, \frac{\Phi_0}{c} \, . \tag{99}$$

There are several way to derive Eq. (99): the easiest is to think that this is just a consequence of the Lorentz force between the current and the magnetic field carried by the vortex [25], or that $\mathbf{f}$ is analogous to the usual Magnus effect, where a lift force acts on a spinning object moving through a fluid. The movement of vortices along y causes in turn an electric field E_x along x that contrasts the applied current, giving rise to power dissipation to maintain a steady state. In particular, E_x can be estimated as follows: each time a vortex drifts across the sample width W, a phase slip of 2π occurs through the sample. The number of vortices that escape the sample in the interval Δt is $n_v v_L \Delta t$, where v_L is the drift velocity of vortices along y and n_v is the (two-dimensional) density of free vortices. Thus the rate of phase slip is

$$\frac{d\Delta\theta}{dt} = 2\pi n_v L v_L \, . \tag{100}$$

Thanks to the Josephson relation $\Delta V = (\hbar/2e)\, d\Delta\theta/dt$, this corresponds to a field $E_x = \Delta V/L$ equal to

$$E_x = \frac{\Phi_0}{c} n_v v_L \, . \tag{101}$$

Notice that Eq. (101) can also be seen as a consequence of Faraday law: as soon as a vortex escapes the sample there is a flux variation of Φ_0, so that the induced electric field is $\mathbf{E} = \mathbf{B}\times\mathbf{v}_L/c$, that corresponds to Eq. (101), with $B = n_v \Phi_0$. In the steady state the drift velocity v_L will be simply proportional to the applied Magnus force (99), so that

$$\mathbf{v}_L = \mu_V \mathbf{f} = -\varepsilon_i \mu_V \frac{j\Phi_0}{c} \, \hat{y} \, , \tag{102}$$

where $\mu_V = D/k_B T$ is the vortex mobility and D is the diffusion constant of vortices. In summary, we obtain that free-vortex motion gives a contribution to the resistivity of the material as

$$\rho = \frac{E_x}{j} = \left(\frac{h}{2e}\right)^2 n_v \mu_V \,. \tag{103}$$

It is worth noting that Eq. (103) is a typical example of duality relation: indeed, the resistivity of the real (electronic) charges is expressed as a "conductivity" of the dual vortex charges $h/2e$, given as usual by the charge squared times the density of charges and their mobility. Eq. (103) can be further simplified by using the Bardeen-Stephen [25] expression for the vortex mobility μ_V, derived by an estimate of the dissipation due to the (normal) vortex core

$$\mu_V = 2\pi\xi_0^2 c^2 \rho_n \Phi_0^2, \tag{104}$$

where ρ_n is the normal-state resistivity and ξ_0 is the correlation length, which sets the size of the vortex core. By inserting Eq. (104) into Eq. (103) one obtains

$$\rho = \rho_n 2\pi\xi_0^2 n_v. \tag{105}$$

All the above discussion assumes that one has a finite density n_v of free vortices. However, below T_{BKT} vortices are bound in pairs, and one would then expect to have zero resistance. Nonetheless, when the applied current is large enough a finite free vortex density n_v can be induced even below T_{BKT}. To understand it, we should consider how the magnus force (99) modifies the interaction energy between vortices that we derived in Eq. (46): in particular, the energy per unit length in a film of thickness d of a vortex-antivortex pair at distance r will now read

$$\frac{E}{d} = \frac{2\pi J_s}{d} \ln\frac{r}{\xi_0} - \mathbf{f}\cdot\mathbf{r} = \frac{2\pi J_s}{d} \ln\frac{r}{\xi_0} - \frac{I}{Wd}\frac{\Phi_0}{c} y. \tag{106}$$

As one can see, the $\log$ potential tends to confine (i.e. bind) the vortexes, while the current tends to unbind them. The energy has a maximum at the scale where its derivative vanishes, i.e., when $\partial E(y^*)/\partial y = 0$, where

$$y^* = \frac{2\pi J_s c W}{I\Phi_0} \,. \tag{107}$$

This means that for separations $y > y^*$ it becomes energetically favorable for a vortex pair to unbind. Since the maximum separation between vortices is cut-off by the sample width W, whenever $y^* > W$ the vortex pair cannot be dissociated within the sample. In contrast, when the current is large enough to get $y^* \leq W$ free vortexes are generated. The minimum current required to unbind the vortices is then such that $y^* = W$, so that

$$I^* = 2\pi J_s \frac{c}{\Phi_0}, \tag{108}$$

and for $I > I^*$ a free vortex density $n_v(I)$ will be present. To estimate it one can use a kinetic-like equation for n_v such that

$$\frac{dn_v}{dt} = \Gamma(T, I) - n_v^2 \tag{109}$$

where Γ is the rate at which vortices are unbound, and can be taken as $e^{-E(y^*)/T}$, where $E(y^*)$ is the energy of a vortex pair at the threshold instability determined above. The second term in

Eq. (109) accounts for the vortices recombining to form pairs again. In the steady state then one has

$$n_V = \Gamma^{1/2} = e^{-E(y^*)/2T}. \tag{110}$$

From Eq. (105) we already established that $\rho \sim n_v$, where $\rho = E_x/j \propto V/I$. We conclude that

$$V \sim n_v I. \tag{111}$$

Let us then estimate n_v by means of Eq. (110). By using the y^* value (107) in Eq. (106) we get

$$E(y^*) = 2\pi J_s \ln \frac{2\pi J_s c W}{\xi_0 \Phi_0 I} - \frac{2\pi J_s c}{d} = 2\pi J_s \ln \frac{I^* W}{I \xi_0} - \frac{2\pi J_s c}{d}\,. \tag{112}$$

Since only the first term depends on the applied current, we obtain from Eq. (110) that the vortex density scales with the current I as

$$n_v = e^{-E(y^*)/2T} \sim e^{-\pi J_s \ln(I^*/I)/T} = \left(\frac{I}{I^*}\right)^{\pi J_s/T}. \tag{113}$$

When replaced into Eq. (111) this implies that above I^* one should observe a non-linear I-V characteristic controlled by the exponent

$$V \propto I^{a(T)}, \quad a(T) = \frac{\pi J_s(T)}{T} + 1\,. \tag{114}$$

From Eq. (73), it follows then that a should jump discontinuously from $a = 3$ at $T = T_{BKT}^-$ to $a = 1$ at $T = T_{BKT}^+$. Below T_{BKT}, the exponent a is expected to increase with decreasing T since the superfluid density increases. The extraction of the superfluid-density jump from the exponent of I-V characteristics has been one of the very first demonstration of BKT physics in thin films of superconductors [8, 9]. Later on, it has been used to characterize the BKT transition in several systems, even when its application can be questioned (see Ref. [41] and discussion therein). The main problem is the identification of the correct range of temperatures and currents where Eq. (114) should be applied. As explained above, non-linearity is expected only *below* T_{BKT} and *above* I^*. In real samples even below T_{BKT} finite-size effects always lead to a finite n_v even for $I \to 0$, that is orders of magnitude smaller than the normal-state one [42]. So the effect of vortex unbinding will manifest in the experiments as a deviation from a linear characteristic to a non-linear one as I overcomes the threshold value I^* for vortex-pair proliferation [13, 41, 42]. To get an idea of its value, one can use the universal relation (73) to replace $2\pi J_s$ with $4k_B T_{BKT}$ in the previous equation. Then using $c/\Phi_0 = 0.5 \cdot 10^{15}$ A / J one has

$$I^*[A] = \frac{c}{\Phi_0} 4 k_B T_{BKT} \simeq 2.67 \cdot 10^{-8}\, T_{BKT}[K] \tag{115}$$

In conventional superconductors where $T_{BKT} \sim 10$ K this corresponds to a current of order of 10^{-7} A. In experiments the crossover is observed for larger currents (usually around 10^{-5} A), an effect that has been ascribed to sample inhomogeneity [42]. However, this also implies that one should avoid to confuse the threshold current for vortex-pair unbinding with the real critical current of the superconductor, where Cooper pairs break down. In Ref. [41] it has been shown how taking into account the effect of inhomogeneity on the smearing of the superfluid-density jump, that we described before, one can get an excellent agreement between the $J_s(T)$ dependence extracted from direct measurements of the inverse penetration depth via two-coils mutual inductance in NbN (see Fig. 4) and the one extracted from the I-V exponent (114). On the other hand, as discussed in Ref. [41], there have been several examples in the literature where the existence of BKT physics has been claimed based on the analysis of I-V non-linearity in a *wrong* temperature/current regime. One paradigmatic example is provided by $SrTiO_3$-based oxide interfaces, where the SC transition has a considerable broadening, that seems to indicate a percolative transition in a network of SC islands of micrometer size, rather that the inhomogeneity on nanometer scales observed in thin films of conventional superconductors, as NbN. In this case non-linear I-V characteristics have been actually measured, but at temperatures *larger* than the real T_c. In Ref. [41] we then argued that in these systems the non-linearity of the I-V characteristics cannot be simply ascribed to vortex-antivortex unbinding triggered by a large current, as it happens within the BKT scheme, since this would lead to dramatically overestimate the BKT transition temperature. In contrast, the observed I-V characteristics can be well reproduced theoretically by modeling the effect of mesoscopic inhomogeneity of the superconducting state, as a consequence of pair-breaking effects in the weaker SC regions, that leads to a progressive non-linear increase of the voltage as the driving current increases, see Fig. 6. In general, one should be very careful in drawing any conclusion about BKT physics for non-linear characteristics measured above the real transition temperature, i.e., the one where resistivity drops to zero (within the available experimental resolution).

7.2 Vortex contribution to transport: paraconductivity

A second possible identification of a BKT transition, still related to vortex transport, is connected to the temperature dependence of the resistivity as one approaches T_{BKT} from above, that can be used to experimentally determine the characteristic exponential divergence of $\xi(T)$ that we derived in Eq. (89) above. As we mentioned, this temperature variation is radically different from the usual power-law divergence (15) observed for ordinary Ginzburg-Landau (GL) fluctuations, where $\xi^2_{GL} \sim T_c/(T - T_c)$ as one approaches T_c from above. The difference between the two regimes can be eventually tested experimentally by extracting the temperature dependence of the so-called paraconductivity, i.e., the contribution of SC (amplitude and phase) fluctuations to the conductivity. Indeed, both within GL and BKT theory [22] the contribution σ_s of SC fluctuations to the normal-state conductivity σ_N diverges as T approaches the transition temperature as ξ^2

$$\frac{\sigma_s}{\sigma_N} = \left(\frac{\xi(T)}{\xi_0}\right)^2. \tag{116}$$

Within GL theory the above result is the consequence of SC fluctuations of the order parameter, that can be technically understood as the so-called Aslamazov-Larkin correction to the bare current-current correlation function with Cooper-pair fluctuations above the critical temperature

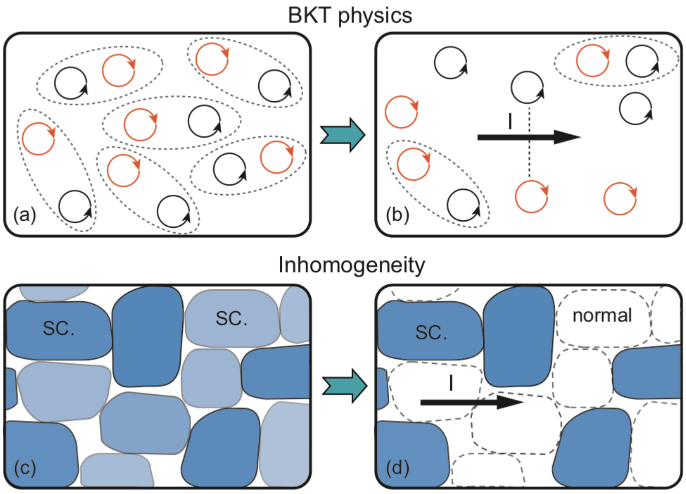

Fig. 6: *Adapted from Ref. [41]. Sketch of the difference between I-V non-linearity arising from BKT physics and from inhomogeneity. In the BKT case, the vortices, which are bound below T_{BKT} in pairs with opposite vorticity (a), get unbound by a sufficiently large current I (b). This generates an extra voltage drop proportional to the average density of unbound vortices, leading to nonlinear characteristics, as given by Eq. (114). In the case of inhomogeneous superconductors, instead, the system segregates into puddles with different strength of the local SC condensate (c). As a consequence, a finite applied current I can turn weak SC puddles into normal ones (d), nonlinearly increasing the global resistivity.*

T_c [43]. The main theoretical paradigm behind this result is the idea that one can describe SC fluctuations above T_c via a Gaussian GL functional, where the fluctuations of the complex order parameter are described by a diffusive mode, that dresses the metallic fermionic response. In this view such Gaussian fluctuations do not distinguish the amplitude from the phase (a distinction that is only possible below T_c), and essentially describe the incipient formation of Cooper pairs with size $\xi(T)$ above T_c. The progressive divergence of σ as $\xi(T)$ increases by approaching T_c, encoded in Eq. (116), is an indication of the formation of fluctuating Cooper pairs with increasing size. As a consequence the resistivity, given by $\rho = 1/(\sigma_N+\sigma_s)$, decreases continuously to zero in the range of temperatures where $\xi(T)$ increases. This effect is then expected to be present regardless of the dimensionality of the system: all non-universal effects, that account for example for the range of temperatures where the paraconductivity can be appreciated experimentally, depend on the specific parameters of the GL functional, that are not universal. A detailed description of GL fluctuations can be found in Ref. [43].

Within the BKT theory one should then expect, as suggested by Halperin and Nelson in [22], that as T decreases one first observes a regime of GL fluctuations, and then a BKT fluctuation regime between the mean-field temperature T_c (that one would observe in the 3D case) and the 2D BKT temperature T_{BKT}. This corresponds to the same range of temperatures where the stiffness is suddenly suppressed by vortex proliferation, as discussed above. To make a correspondence between the GL and the BKT result for the paraconductivity let us go back to Eq. (105) above, where we established a general relation between the dissipative motion of free vortices and the vortex density n_v. While in the previous Section we derived the vortex density induced below T_{BKT} by a large current $n_v(I)$, above T_{BKT} we already have a finite $n_v(T)$ due to the thermal dissociation of vortex-antivortex pairs. In particular, since ξ is the scale where the superfluid density vanishes above T_{BKT}, we can identify

$$n_v \equiv \frac{1}{2\pi\xi^2(T)} \tag{117}$$

so that from Eq. (105) we obtain exactly the form (116), provided that $\xi(T)$ is given by eq. (89). In principle, the experimental determination of such exponential behavior via paraconductivity measurements could represent a clear signature of BKT physics. However, as the above discussion demonstrates, the validity of Eq. (89) is limited to a narrow range of temperatures between T_c and T_{BKT}. In addition, the value of the parameters appearing in the BKT correlation length $\xi \sim ae^{-b/\sqrt{t}}$ are *not* arbitrary, since they depend on the distance (92) between T_c and T_{BKT}, as originally discussed in Ref. [22], and on the value μ of the vortex-core energy, as more recently discussed in Ref. [42], where it has been shown that

$$b = 2\frac{\mu}{\mu_{XY}}\sqrt{\frac{T_c - T_{BKT}}{T_{BKT}}}. \tag{118}$$

For conventional superconductors, such as NbN, usually $\sqrt{\frac{T_c - T_{BKT}}{T_{BKT}}} \sim 0.1$, while $\mu/\mu_{XY} \sim 0.5$, as estimated by the fit of $J_s(T)$ in [10]. In general, all these parameters are constrained one to the other. However, it is not uncommon in the literature that a fit to the resistivity $\rho(T)$ above T_c is attempted with a BKT formula like Eq. (116), without a check a-posteriori that the obtained b value is consistent with its expression via Eq. (118). Some examples of potential problems of this kind are discussed in Ref. [42, 41].

8 Conclusions

In this lecture I gave an introductory overview on the properties of the BKT transition, as it was originally formulated within the classical XY-model, the Coulomb-gas model and the sine-Gordon model. The mapping among these physically different problems turned out to be useful for the analytical derivation of various properties, including the celebrated RG equations. The two most spectacular effects obtained by the RG equations are the universal and discontinuous jump of the superfluid stiffness as the transition is approached from below, and the exponential divergence of the correlation length as the transition is approached from above. I then discussed how these rather specific signatures can be observed in real materials, focusing in particular on the case of superconducting systems. My personal view after several years of intense work in close connection with experiments is that BKT physics has been clearly observed in some cases, but often in the literature the observation of BKT signatures has been based on a naive application of the celebrated BKT formulas. This caveat should be taken by the readers to develop a critical attitude towards the identification of BKT signatures in experiments.

Appendix

A Averages over Gaussian variables

To understand Eq. (11) let us consider a generic Gaussian model with real variables $u(r) \equiv (1/\Omega)\sum_{\mathbf{q}} e^{i\mathbf{q}\cdot\mathbf{r}} u_{\mathbf{q}}$ (where Ω is the volume) whose Hamiltonian in momentum space reads

$$H = \frac{1}{2}\sum_{\mathbf{q}} G(q)\,|u_{\mathbf{q}}|^2. \tag{119}$$

To compute the partition function let us define the integrals over the complex variables $u_{\mathbf{q}}$ in the usual way

$$\int \frac{du_{\mathbf{q}} du^*_{\mathbf{q}}}{2\pi i} \quad e^{-au_{\mathbf{q}}u^*_{\mathbf{q}}} \equiv \int \frac{d\,\mathrm{Re}\,u_{\mathbf{q}}\,d\,\mathrm{Im}\,u_{\mathbf{q}}}{\pi} e^{-au_{\mathbf{q}}u^*_{\mathbf{q}}} = \frac{1}{a}, \tag{120}$$

$$\int \frac{du_{\mathbf{q}} du^*_{\mathbf{q}}}{2\pi i}\, u_{\mathbf{q}}u^*_{\mathbf{q}} e^{-au_{\mathbf{q}}u^*_{\mathbf{q}}} = \quad \frac{1}{a^2}. \tag{121}$$

Since we have only N independent $u(r)$ variables we use the relation $u^*_{\mathbf{q}} = u_{-\mathbf{q}}$ to halve the number of allowed $\mathbf{q}$ values in Eq. (119), so that

$$H = \frac{1}{\Omega}\sum_{\mathbf{q}>0} G(q)\big((\mathrm{Re}\,u_{\mathbf{q}})^2 + (\mathrm{Im}\,u_{\mathbf{q}})^2\big), \tag{122}$$

where we used the symbolic short-hand notation "$\mathbf{q} > 0$". We can then easily compute the partition function as

$$Z = \int \mathcal{D}u\, e^{-\beta H[u]} = \prod_{\mathbf{q}>0}\left(\frac{\Omega}{\beta G(\mathbf{q})}\right), \tag{123}$$

while the average values read

$$\langle u_{\mathbf{q}} u_{\mathbf{q}'}\rangle = \delta_{\mathbf{q}+\mathbf{q}'}\,\frac{\Omega}{\beta G(\mathbf{q})}\,. \tag{124}$$

Finally, one can easily get the average values of exponential of linear functions in the u variables. Indeed, if we define in general

$$R(\mathbf{r}) = \frac{1}{\Omega}\sum_{\mathbf{q}} u_{\mathbf{q}}\, C_{-\mathbf{q}}(\mathbf{r}), \tag{125}$$

we see that

$$\begin{aligned}\left\langle e^{iR(r)}\right\rangle &= \frac{1}{Z}\int \mathcal{D}u\, e^{-\frac{1}{\Omega}\sum_{\mathbf{q}>0} G(q)u_{\mathbf{q}}u_{-\mathbf{q}} + \frac{i}{2\Omega}\sum_{\mathbf{q}>0} u_{\mathbf{q}}C_{-\mathbf{q}}(\mathbf{r}) + \frac{i}{2\Omega}\sum_{\mathbf{q}>0} u_{-\mathbf{q}}C_{\mathbf{q}}(\mathbf{r})} \\ &= \frac{1}{Z}\int \mathcal{D}u\, e^{-\frac{1}{\Omega}\sum_{\mathbf{q}>0} G(q)[u_{\mathbf{q}} - iC_{\mathbf{q}}/2G(q)][u_{-\mathbf{q}} - iC_{-\mathbf{q}}/2G(q)]} e^{-\frac{1}{2\Omega}\sum_{\mathbf{q}}\frac{C_{\mathbf{q}}C_{-\mathbf{q}}}{G(q)}} = e^{-\frac{1}{2}\langle [R(r)]^2\rangle}\end{aligned} \tag{126}$$

References

[1] V.L. Berezinsky, Sov. Phys. JETP **34**, 610 (1972)

[2] J.M. Kosterlitz and D.J. Thouless, J. Phys. C **6**, 1181 (1973)

[3] J.V. José: *40 Years of Berezinskii-Kosterlitz-Thouless Theory* (World Scientific, Singapore, 2013)

[4] M.H.W. Chan, A.W. Yanof, and J.D. Reppy. Phys. Rev. Lett., **32** 1347, (1974)

[5] D. McQueeney, G. Agnolet, and J.D. Reppy. Phys. Rev. Lett., **52** 1325, (1984)

[6] Z. Hadzibabic, P. Kruger, M. Cheneau, B. Battelier, and J. Dalibard, Nature, **44**, 1118 (2006)

[7] P.A. Murthy, I. Boettcher, M. Holzmann L. Bayha, D. Kedar, M. Neidig, M.G. Ries, A.N. Wenz, G. Zurn, and S. Jochim. Phys. Rev. Lett., **115**, 010401 (2015)

[8] K. Epstein, A.M. Goldman, and A.M. Kadin, Phys. Rev. Lett. **47**, 534 (1981)

[9] A.T. Fiory, A.F. Hebard, and W.I. Glaberson. Phys. Rev. B **28**, 5075, (1983)

[10] A. Kamlapure, M. Mondal, M. Chand, A. Mishra, J. Jesudasan, V. Bagwe, L. Benfatto, V. Tripathi and P. Raychaudhuri, Appl. Phys. Lett. **96**, 072509 (2010); M. Mondal, S. Kumar, M. Chand, A. Kamlapure, G. Saraswat, G. Seibold, L. Benfatto, P. Raychaudhuri, Phys. Rev. Lett. **107**, 217003 (2011)

[11] I. Hetel, T.R. Lemberger and M. Randeria, Nat. Phys. **3**, 700 (2007)

[12] Jie Yong, M.J. Hinton, A. McCray, M. Randeria, M. Naamneh, A. Kanigel, and T.R. Lemberger, Phys. Rev. B **85**, 180507(R) (2012)

[13] P.G. Baity, Xiaoyan Shi, Zhenzhong Shi, L. Benfatto, and Dragana Popovic, Phys. Rev. B **93**, 024519 (2016)

[14] J.A. Bert, K.C. Nowack, B. Kalisky, H. Noad, J.R. Kirtley, C. Bell, H.K. Sato, M. Hosoda, Y. Hikita, H.Y. Hwang, and Kathryn A. Moler. Phys. Rev. B (R) **86**, 060503 (2012)

[15] A. Caviglia *et al.*, Nature **456**, 624 (2008)

[16] S. Mallik, G. Menard, G. Saiz, H. Witt, J. Lesueur, A. Gloter, L. Benfatto, M. Bibes, and N. Bergeal, Nat. Comm. **13**, 4625 (2022)

[17] Y. Saito, Y. Kasahara, J. Ye, Y. Iwasa, and and T. Nojima, Science **350**, 409 (2015)

[18] T. Giamarchi: *Quantum physics in one dimension* (Clarendon Press, 2004)

[19] L. Benfatto, C. Castellani and T. Giamarchi, Phys. Rev. Lett. **99**, 207002 (2007)

[20] L. Benfatto, C. Castellani and T. Giamarchi: *Beresinskii-Kosterlitz-Thouless transition within the sine-Gordon approach: the role of the vortex-core energy*, in [3]

[21] D.R. Nelson and J.M. Kosterlitz, Phys. Rev. Lett. **19**, 1201 (1977)

[22] B.I. Halperin and D.R. Nelson, J. Low Temp. Phys. **36**, 590 (1979)

[23] N.D. Mermin and H. Wagner. Phys. Rev. Lett., **17**, (1966)

[24] N. Nagaosa: *Quantum field theory in condensed matter physics* (Springer, 1999)

[25] M. Tinkham: *Introduction to Superconductivity* (Dover Publications, New York, 2004)

[26] J.M. Kosterlitz, J. Phys. C: Solid State Phys. **7**, 1046 (1974)

[27] V. Ambegaokar, B.I. Halperin, D.R. Nelson, and E.D. Siggia, Phys. Rev. B **21**, 1806 (1980)

[28] P. Coleman: *Introduction to Many-Body Physics* (Cambridge University Press, 2016)

[29] V. Emery and S. Kivelson, Nature **374**, 434 (1995)

[30] L. Benfatto, A. Toschi, and S. Caprara, Phys. Rev. B. **69**, 184510 (2004)

[31] P.W. Anderson, Phys. Rev. **112**, 1900 (1958)

[32] Ilaria Maccari, Lara Benfatto, and Claudio Castellani, Phys. Rev B **99**, 104509 (2019)

[33] S. Doniach and B.A. Huberman, Phys. Rev. Lett. **42**, 1169, (1979)

[34] J. Pearl, Appl. Phys. Lett. **5**, 65, (1964)

[35] S.J. Turneaure, E.R. Ulm, and T.R. Lemberger, J. Appl. Phys. **79**, 4221, (1996)

[36] I. Maccari, L. Benfatto and C. Castellani, Phys. Rev. B **96**, 060508 (2017)

[37] A.B. Harris, J. Phys. C **7**, 1671 (1974)

[38] C.R. Hu, Phys. Rev. B **6**, 1756 (1972)

[39] S. Alama and A.J. Berlinsky, and L. Bronsard and T. Giorgi, Phys. Rev. B **60**, 6901 (1999)

[40] M. Chand, G. Saraswat, A. Kamlapure, M. Mondal, S. Kumar, J. Jesudasan, V. Bagwe, L. Benfatto, V. Tripathi, P. Raychaudhuri, Phys. Rev. B **85**, 014508 (2012)

[41] G. Venditti, J. Biscaras, S. Hurand, N. Bergeal, J. Lesueur, A. Dogra, R.C. Budhani, M. Mondal, J. Jesudasan, P. Raychaudhuri, S. Caprara, and L. Benfatto, Phys. Rev. B **100**, 064506 (2019)

[42] L. Benfatto, C. Castellani, and T. Giamarchi, Phys. Rev. B **80**, 214506 (2009)

[43] Anatoly Larkin and Andrei Varlamov: *Theory of Fluctuations in Superconductors* (Clarendon, Oxford, 2005)